(12) INTERNATIONAL APPLICATION PUBLISHED UNDER THE PATENT COOPERATION TREATY (PCT)

(19) World Intellectual Property Organization
International Bureau

(43) International Publication Date
1 November 2001 (01.11.2001)

PCT

(10) International Publication Number
WO 01/82099 A1

(51) International Patent Classification[7]: G06F 17/00

(21) International Application Number: PCT/GB00/01675

(22) International Filing Date: 2 May 2000 (02.05.2000)

(25) Filing Language: English

(26) Publication Language: English

(30) Priority Data:

9910019.0	1 May 1999 (01.05.1999)	GB
9916499.8	15 July 1999 (15.07.1999)	GB
9919677.6	20 August 1999 (20.08.1999)	GB
9923110.2	1 October 1999 (01.10.1999)	GB
0003711.9	17 February 2000 (17.02.2000)	GB

(71) Applicant *(for all designated States except US)*: **THE COURT OF NAPIER UNIVERSITY** [GB/GB]; Merchiston Tower, Colinton Road, Edinburgh EH10 5DT (GB).

(72) Inventors; and

(75) Inventors/Applicants *(for US only)*: **ADDISON, Paul, Stanley** [GB/GB]; 58 Buckstone Crook, Edinburgh EH10 6UR (GB). **WATSON, James, Nicholas** [GB/GB]; 34 Fowler Terrace, Edinburgh EH11 1DA (GB).

(74) Agent: **MURGITROYD & COMPANY**; 373 Scotland Street, Glasgow G5 8QA (GB).

(81) Designated States *(national)*: AE, AL, AM, AT, AU, AZ, BA, BB, BG, BR, BY, CA, CH, CN, CR, CU, CZ, DE, DK, DM, EE, ES, FI, GB, GD, GE, GH, GM, HR, HU, ID, IL, IN, IS, JP, KE, KG, KP, KR, KZ, LC, LK, LR, LS, LT, LU, LV, MA, MD, MG, MK, MN, MW, MX, NO, NZ, PL, PT, RO, RU, SD, SE, SG, SI, SK, SL, TJ, TM, TR, TT, TZ, UA, UG, US, UZ, VN, YU, ZA, ZW.

(84) Designated States *(regional)*: ARIPO patent (GH, GM, KE, LS, MW, SD, SL, SZ, TZ, UG, ZW), Eurasian patent (AM, AZ, BY, KG, KZ, MD, RU, TJ, TM), European patent (AT, BE, CH, CY, DE, DK, ES, FI, FR, GB, GR, IE, IT, LU, MC, NL, PT, SE), OAPI patent (BF, BJ, CF, CG, CI, CM, GA, GN, GW, ML, MR, NE, SN, TD, TG).

Published:
— *with international search report*

For two-letter codes and other abbreviations, refer to the "Guidance Notes on Codes and Abbreviations" appearing at the beginning of each regular issue of the PCT Gazette.

(54) Title: METHOD OF ANALYSIS OF MEDICAL SIGNALS

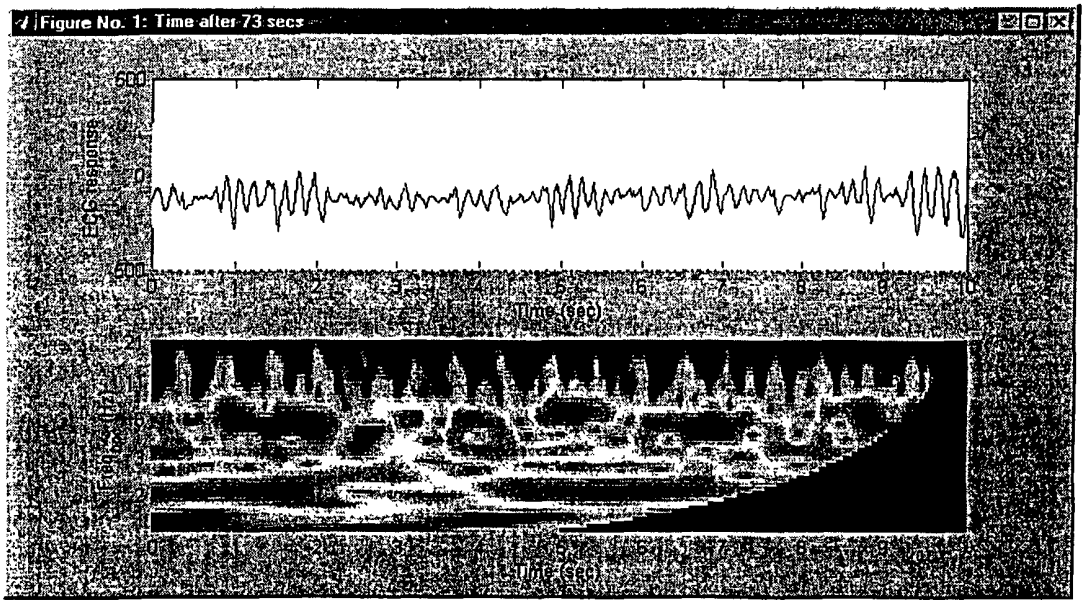

(57) Abstract: A method of analysis of medical signals which uses wavelet transform analysis to decompose cardiac signals. Apparatus for carrying out the method, and cardiac apparatus adapted to employ the method are also described.

WO 01/82099 A1

"Method of Analysis of Medical Signals"

This invention relates to a method of analysis of medical signals, and in particular to a method of decomposition of cardiac signals using wavelet transform analysis. Specifically the invention relates to an improved method of resuscitation of patients in cardiac arrest.

In the UK, coronary heart disease is the second greatest contributor to deaths of people under 75. The social and economic consequences of these death rates

are enormous. The current survivability rates of patients after sudden cardiac failure are around 1:10.

Ventricular tachyarrhythmias, specifically ventricular fibrillation (VF), are the primary arrhythmic events in cases of sudden cardiac death. Administration of prompt therapy to a patient presenting with such symptoms can however lead to their successful resuscitation. Until recently, the only indicators of likelihood of survival of a patient to hospital discharge were traditional variables such as emergency service response time or bystander cardio-pulmonary resuscitation (CPR).

In most cardiac complaints, analysis of a surface electrocardiogram (EKG) of the presenting patient is a rich source of information. However, until recently, a surface EKG recorded during VF and any subsequent medical intervention to defibrillate, was thought merely to present unstructured electrical activity, and not to provide useful information.

The first attempts to derive prognostic information from EKGs of the heart in VF focussed on the importance of the amplitude of the waveform defined using peak-to-trough differences in the EKG voltage, measured as either the greatest deflection occurring in a predefined time slot, or as the average peak-to-trough voltage measured over a given time interval. It has been shown that the VF amplitude is inversely related to time elapsed since collapse, is a crude predictor of defibrillation outcome, and is a better indicator of

survival to hospital discharge than the traditional variables described above.

However, recording the VF amplitude accurately is significantly problematical. The EKG voltage amplitude measured during VF is dependent on the direction of the main fibrillation vector and is influenced by a variety of factors including patient chest shape; electrode size; electrode location; and skin/electrode interface resistance. This number of variables makes this amplitude measure both unreliable and inaccurate. That is, although the amplitude of the waveform of an EKG recorded during VF is now recognised to be a crude predictor of the likely outcome of resuscitation of a patient in VF, it is not a reproducible marker of sensitivity to defibrillation, and lacks clinical usefulness.

In a further development, it is also known to use Fast-Fourier based transforms to generate a frequency spectrum of an EKG in VF to analyse the signal. The median frequency (MF) divides the area under the spectrum into two equal parts. Since this plot is derived from information in both the voltage and time domains, external variables such as lead placement have less effect on the results than the method of observing the amplitude. However, CPR produces artefacts in the recorded EKG signal and, since pausing CPR merely to obtain an EKG signal free of artefacts is likely to compromise resuscitation, these artefacts are necessarily included in this frequency measure, and detract from its usefulness.

Thus the results of such signal analysis show some correlation with the likely outcome of resuscitation, but again lack sufficient sensitivity and specificity for clinical use. That is, this form of analysis has the disadvantage that, since the Fourier spectrum contains only globally averaged information, specific features in the signal are lost.

A method of accurate analysis of a surface EKG waveform recorded during VF would therefore be useful in understanding the pathophysiological processes in sudden cardiac death, and thus to produce a model for use:

in predicting the efficacy of therapy in individual cases; and

in determining the selection of the preferred course of primary, and alternative or adjunct therapies thus providing a means for individually tailored therapy for the specific patient needs

to improve the success rate of resuscitation of patients presenting in VF.

Atrial fibrillation (AF) is a common cardiac arrhythmia in older people. Atrial fibrillation can be stopped by giving an electric shock to the patient under general anaesthetic (cardioversion). However, many patient return to an AF rhythm soon after treatment. The technology detailed here may also provide a tool to

facilitate the clinical evaluation of AF exhibited in the electrocardiogram (EKG) so reducing the risk associated with general anaesthetic in patients where the applied therapy is likely to prove ineffective.

According to the present invention there is provided a method of decomposition of waveforms in a cardiac signal using wavelet transform analysis.

The method of the invention is non-invasive, accurate, and capable of delivering real-time information.

Preferably said method employs discretized wavelet transform analysis to process the EKG.

Preferably said method employs discretized continuous wavelet transform analysis to process the EKG.

Preferably said method comprises the steps of deriving the wavelet energy surfaces of an EKG signal; and plotting said wavelet energy surfaces against a location parameter b, and a scale parameter. The scale parameter may be dilation a or band pass frequency f_{bpc}.

The method initially comprises the steps of connecting electrodes to the presenting patient; and sampling the analogue input signal to derive the cardiac signal.

Typically said method comprises the step of visually displaying the cardiac signal.

Said method may display the distribution of energies within the cardiac signal. Said method may display coherent structures within the cardiac signal.

Said display may be by means of a contour plot. Said display may be by means of a surface plot. Preferably said method provides means to visualise the signal in real-time for clinical use.

Preferably said method is applicable in the analysis of an EKG in ventricular fibrillation.

Said method may be applicable in the analysis of an EKG in ventricular fibrillation after the commencement of cardio-pulmonary resuscitation (CPR).

The method may include the step of disassociating the component features of the temporal trace of a recorded EKG. Additionally or alternatively said method may include the step of temporal filtering of an EKG signal of a heart which is subject to CPR to disassociate the CPR signal from the heart signal.

Typically said method provides measurable characteristics for the estimation of the health of a heart in VF. Said method may provide measurable characteristics for the estimation of the health of a heart in AF. Said me may provide Typically said method provides measurable characteristics for the estimation of the health of a heart.

The method may provide measurable characteristics for the estimation of the time elapsed since the onset of a cardiac incident.

Typically said method provides measurable characteristics for the estimation of the health of a heart after commencement in CPR.

Said method may provide a prediction for the outcome of a given therapeutic intervention and so aid the clinical decision making process.

Said method may provide a basis for individual, patient specific, protocols for therapeutic intervention.

The method may provide a guide to the optimal timing of defibrillation of a heart in VF.

Said method may include the step of constructing a damage index for reference purposes. Construction of said index might involve the development of a network classifier from a library of recorded data. Said network classifier may comprise a neural network. Said network classifier may comprise a wavelet network classifier.

Application of the method of the invention represents a significant advance in coronary care by providing a reliable predictor of the outcome of shocking a patient in VF. In addition, the development of an algorithm using the method of the invention gives the ability to predict shock outcome and to facilitate individual

patient therapy. The ability to provide patient specific therapeutic intervention is a priority in the advancement of currently applied medical protocols.

That is, as discussed above, in certain instances, after prolonged cardiac arrest preceding defibrillation pharmacological measures or CPR can increase the chance of successful resuscitation. Thus, employing the method to predict the outcome of shocking avoids futile defibrillation attempts which can even harm the heart, and can indicate the need for intervention, and influence the selection of the preferred type of intervention, to optimise the metabolic state of the heart prior to counter-shock.

The predictor algorithm developed using the method is being tested using a new generation of defibrillation devices that have the flexibility to allow easy prototyping of the new defibrillation algorithms.

According to a further aspect of the present invention there is provided a method of decomposition of waveforms in a cardiac signal using matching pursuit algorithms.

According to a further aspect of the present invention there is provided an apparatus for decomposition of waveforms in a cardiac signal, said apparatus comprising wavelet transform analysis means.

Said apparatus may include means to display the distribution of energies within a waveform.

Said apparatus may include a monitor adapted to display decomposed waveforms. Said apparatus may be adapted for inclusion in an EKG apparatus.

According to a further aspect of the present invention there is provided defibrillation means adapted to operate in response to a signal generated by comparison of an EKG trace with decomposed waveform.

That is, the invention preferably provides a method of wavelet analysis of cardiac signals which provides structural information about the heart - whether the heart is healthy or not - and has significant advantages over fast Fourier transforms.

The invention may provide a display device in the form of a scrologram that provides real-time visualisation of a wavelet scalogram, showing the distribution of energies and coherent structures within the signal for use as guidance by a clinician.

The invention may further provide a data analysis tool, which assists in shock timing (atrial pulsing). That is, the derived data may indicate the optimum time to administer shock to the heart. The invention may provide a damage index, preferably in the form of an artificial neural network.

Preferably the invention provides dissociation of the component features of a temporal trace of a cardiac signal, which may for example be CPR, AF, or cardio-phonographic signals.

Embodiments of the invention will now be described by way of example only and with reference to the accompanying drawings in which:

Figure 1a is a Mexican hat wavelet;

Figure 1b is the real part of a complex Morlet wavelet;

Figure 2a is a schematic plot showing the dilation of a continuous wavelet;

Figure 2b is a schematic plot showing the translation of a continuous wavelet;

Figures 3a to Figure 3e are the plots of the 'investigation' of a sinusoidal signal by Mexican hat wavelets of various sizes, showing the effect of translation of the wavelet along the signal (change in b), and dilation of the wavelet (change in a);

Figure 4a is the plot of five cycles of a sine wave of period P;

Figure 4b is the contour plot of $T(a,b)$ against a and b for the sine wave of Figure 4a;

Figure 4c is the isometric surface plot of $T(a,b)$ against a and b for the sine wave of Figure 4a;

Figure 5a is the plot of a combination of two sine waves of period P1, and P2, where P1 = 5P2;

Figure 5b is the contour plot of *T(a,b)* against *a* and *b* for the sine wave of Figure 5a;

Figure 5c is the isometric surface plot of *T(a,b)* against *a* and *b* for the sine wave of Figure 5a;

Figure 6a is an EKG trace of a pig heart in sinus rhythm;

Figure 6b is a 2D energy scalogram associated with the EKG trace of Figure 6a;

Figure 6c is a 3D energy scalogram associated with the EKG trace of Figure 6a;

Figures 6d, 6e, 6f and 6g are the energy surface plots from four segments of an EKG signal subsequent to the onset of VF, showing the three dominant ridges A, B, and C appearing in the transform surface, and showing in Figure 6g the onset of CPR after five minutes, associated with a gradual increase in passband frequency of the ridges A,B, and C;

Figure 7a is an energy scalogram for a pig heart for the first seven minutes of ventricular fibrillation, indicating the initiation of CPR after five minutes;

Figure 7b is a schematic diagram of the salient features of the scalogram of Figure 7a;

Figure 7c is the smoothed plot of energy at the 8Hz level in the scalogram of Figure 7a against time;

Figure 8a is a typical segment of an EKG trace of a pig heart in VF;

Figures 8b, 8c, and 8d are the energy scalograms associated with the trace of Figure 8a;

Figure 9 is a screen shot of a real time viewer which shows the collected EKG data with its associated wavelet energy display in the form of its energy scalogram, where windows scroll to the right;

Figure 10a is a 7 second trace of human ECG showing a shock event;

Figure 10b is a scalogram corresponding to the trace of Figure 10a;

Figure 11a shows the proportion of energy in scalograms for 120 results (60 ROSC, and 60 asystole) at 1.9 Hz after shocking;

Figure 11b shows the proportion of energy in scalograms for 120 results (60 ROSC, and 60 asystole) at 9.3 Hz after shocking;

Figure 12a is a schematic representation of overlapping signal segments used in a neural network test study;

Figure 12b shows the weights attributed by the Kohonen network to the 30 frequency levels used in the scalogram;

Figure 13a is an aorta pressure trace;

Figure 13b shows the EKG for the same time period as the trace of Figure 13a; and

Figure 13c is the scalogram associated with the trace of Figure 13a derived from the Morlet wavelet;

Figure 13d is a detail of the phase part of scalogram Figure 13c;

Figure 13e is the scalogram associated with the trace of Figure 13a derived from the Mexican hat wavelet; and

Figure 13f demonstrates the correlation of aorta pressure pulse position with lines of zero phase;

Figures 14a is the plot of an EKG trace. Figure 14b is its associated phase at around 1.5Hz. Figure 14c is its energy scalogram. The correlation of zero phase at this lower frequency

and high frequency (low dilation) peaks is thus illustrated.

Figure 15a shows a 2 second segment of EKG taken from a patient with atrial fibrillation (AF). Figure 15b shows the wavelet scalogram plot associated with this EKG. Figure 15c shows the corresponding modulus maxima of the scalogram of Figure 15b.

Figure 15d contains a 7 second segment of EKG exhibiting AF. Figure 15e is a trace of EKG temporal components with small amplitude. Figure 15f shows the larger magnitude components i.e. the QRS and T waves.

Figure 15g is a plot of a two second 'blow up' of part of the signal of Figure 15d; Figure 15h is a plot of a two second 'blow up' of part of the signal of Figure 15e; and Figure 15i is a plot of a two second 'blow up' of part of the signal of Figure 15f.

Referring to the Figures, the present method employs the use of a wavelet transform to analyse a cardiac signal.

The method involves the decomposition of the signal. This decomposition is accomplished by utilising wavelet transforms to decompose the signal in wavelet space.

A key distinction between the Fourier analysis of an EKG signal and its analysis by means of a wavelet function is that, whilst the Fourier transform employs a sinusoid function, a wavelet function is localised in time.

The methodology for such decomposition may include discretized continuous wavelet transforms, orthonormal wavelet transforms of decimated construction, non-decimated wavelet transforms, wavelet packet transforms and matching pursuit algorithms.

Signal processing employing wavelet transform analysis allows simultaneous elucidation of both spectral and temporal information carried within a signal. Such processing can employ either continuous or discrete transforms. The choice of wavelet transform used for a particular signal processing application depends on factors such as speed of computation necessary, the shape of signal specific features, the frequency resolution required, and the statistical analysis to be performed.

The preferred method employs the discretized continuous transform as it provides high resolution in wavelet space at lower frequencies.

This method thus employs the use of a discretized continuous wavelet transform to analyse a cardiac signal.

In particular, this method employs a wavelet transform as an interrogation tool for EKG signals of ventricular fibrillation.

A variety of wavelet functions are available, and the most appropriate is selected to analyse the signal to be investigated.

The wavelet transform of a continuous time signal, $x(t)$, is defined as:

$$T(a,b) = \frac{1}{w(a)} \int_{-\infty}^{\infty} x(t) \overline{g}\left(\frac{t-b}{a}\right) dt \qquad \text{equation 1}$$

where $g(t-b)/a)$ is the analysing wavelet function and '$\overline{\ }$' denotes complex conjugate. $w(a)$ is a scaling function usually of the form $w(a)=a^n$ where n is usually 1 or 0.5, and $x(t)$, in this application, is the single channel surface EKG time signal. The transform coefficients $T(a,b)$ are found for both specific locations on the signal, b, and for specific wavelet dilations, a. $T(a,b)$ is plotted against a and b in either a surface or contour plot.

While other wavelet types may be employed the wavelets mainly used in this method are: the Mexican hat wavelet and the Morlet wavelet, examples of which are shown in Figure 1.

The wavelet can translate along the signal (change in *b*) and dilate (change in *a*). This is shown schematically in Figure 2 using a Mexican hat wavelet.

Figure 3 illustrates the way in which a sinusoidal signal can be 'investigated' at various locations by Mexican hat wavelets of various sizes. The numerical value of the convolution (equation 1) depends upon both the location and dilation of the wavelet with respect to the signal.

Figure 3a shows a wavelet of similar 'size' to the sinusoidal waves superimposed on the signal at a *b* location which produces a reasonable matching of the wavelet and signal locally. From the Figure it is apparent that there is a high correlation between the signal and wavelet at this *a* scale and *b* location. Here, the cross correlation of the signal with the wavelet produces a large positive number *T(a,b)*.

Figures 3b and 3c show details of the wavelet transform of a signal using a wavelet of approximately the same shape and size as the signal in the vicinity of *b*. Figure 3b shows a wavelet of similar scale to the sinusoidal waveform located at maximum negative correlation. This produces a large negative *T(a,b)* value. Figure 3c shows a wavelet of similar scale to the sinusoidal waveform located at a position on the time axis where near zero values of *T(a,b)* are realised. Figure 3d shows the effect on the transform of using the smaller *a* scale. It can be seen from the plot that the positive and negative parts of the wavelet are all in the vicinity of approximately the

same part of the signal, producing a value of *T(a,b)* near zero. Figure 3e shows that the same thing happens when using a much larger wavelet, since the wavelet transform now covers various positive and negative repeating parts of the signal, again producing a near zero value of *T(a,b)*.

Wavelet transforms are not usually computed at arbitrary dilations for isolated locations in the signal, but rather over a range of *a* and *b*. A plot of *T(a,b)* versus *a* and *b* for sinusoidal data using the Mexican hat wavelet is shown in Figure 4. Two methods are then employed to plot *T(a,b)*, namely a contour plot or *scalogram* as shown in Figure 4b, and a surface plot as shown in Figure 4c. At small and large values of *a*, the near zero values of *T(a,b)* are evident from the plots, but at values of *a* of the order of one quarter of the wavelength of the sinusoid large undulations in *T(a,b)* correlate with the sinusoidal forms of the signal.

Figure 5a shows two superpositioned sinusoidal waveforms, the first with period P1, the second with period P2. P1 = 5P2. Figures 5b and 5c, the transform plots of the superimposed waveforms clearly show the two periodic waveforms in the signal at scales of one quarter of each period. Thus, Figure 5 clearly demonstrates the ability of the continuous wavelet transform to decompose the signal into its separate

frequency components. That is, this transform 'unfolds' the signal to show its constituent waveforms.

The contribution to the signal energy at a specific *a* scale and *b* location is proportional to the two-dimensional wavelet energy density function which is, in turn, proportional to the modulus of $T(a,b)$.

The method of the present invention thus involves the display of the transform as a contour plot. That is, the method is used to present information derived from an EKG trace of the heart in VF as a scalogram. The preferred form of presenting the information is as an *energy scalogram*, which presents the results as a plot showing the log of the wavelet energy coefficients, against the log of the bandpass centre frequency, f_{bpc}, of the wavelets for each time increment. The bandpass centre frequency is proportional to the reciprocal of the dilation value, *a*. This plot highlights small changes in amplitude over the scales of interest. The transform copes with repeating features in time with shifting phase, making it appropriate for real time applications such as this.

That is, by performing continuous wavelet transform analysis on the ECG in VF, and then by producing an *energy scalogram* of the results, it is possible to unfold the signal in such a way that a previously hidden structure is apparent, in contrast to the apparently disorganised VF signal.

The method then includes quantifying the wavelet decomposition. This wavelet decomposition provides both qualitative visual and measurable features of the EKG in wavelet space.

In practice, surface EKG tracings, recorded as soon as possible after the onset of VF, are analysed.

As a demonstration of the efficacy of the method, in an example of an experimental procedure utilising this method of analysis employing wavelet techniques, VF was induced in anaesthetised pigs via a pacemaker probe, using a 90V impulse at 60 Hz. All of the pigs remained in VF, untreated for a period of either 3 or 5 minutes. After this time, CPR commenced. The surface EKG (standard lead II) was recorded using needle electrodes. The EKG was sampled at 300 Hz using a 12-bit A to D converter. The method of the present invention was then performed using 32 EKG tracings recorded immediately after the onset of VF.

Figure 6a represents 4 beats of a pig heart in sinus rhythm. Figures 6b and 6c shows the wavelet transform of the signal displayed in two and three dimensions respectively.

The QRS complex of the waveform is evident from the conical structures in Figure 6b converging to the high frequency components of the RS spike. The P and T waves are also labelled in the plot. The 3D landscape plot of Figure 6c shows the morphology of the signal in

wavelet space. In Figures 6b and 6c the continuous horizontal band *(X)* is associated with a frequency of 1.7 Hz, the beat frequency of the sinus rhythm. The second band *(Y)* occurs at a frequency of approximately 5.1 Hz, corresponding to the separation of the P-QRS-T components in time. At higher frequencies the P, QRS and T components are individually resolved according to their frequency makeup and temporal location.

Figures 6d to 6g show the energy surfaces for four segments of EKG signal subsequent to the onset of VF, namely: (6d) 0-60 s; (6e) 60-100 s; (6f) 210-240 s; and (6g) 260-360 s.

The morphology of the VF signal in wavelet space can be seen from the Figures to contain underlying features within a more complex surface topography. The most significant features are the dominant ridges that appear in the transform surface through time.

Figure 6f shows these ridges quite clearly. A high-energy ridge can be observed at around 10 Hz and two lower energy bands can be observed at lower frequencies. These three ridges are labelled A, B and C, respectively, in the plot. Other ridges are also present within the scalogram.

The energy surface in Figure 6g contains the onset of CPR after 5 min of untreated VF. The institution of CPR is associated with a gradual increase in the passband frequencies of ridges A, B and C. This change in the composition of the VF signal reflects electrical

changes in the fibrillating myocardium associated with the onset of CPR. This is because CPR produces antegrade myocardial blood flow and thus improves the metabolic state of the tissues, temporarily reversing the otherwise progressive decline in high band pass frequency components of the EKG wavelet decomposition.

Figure 8a is a typical segment of an EKG trace of a pig heart in VF; Figures 8b, 8c, and 8d are the energy scalograms associated with the trace of Figure 8a. As clearly illustrated by these diagrams the principle dilation (band pass centre frequency) component of the scalogram is approximately 10Hz. However, using said method it is also apparent that this component is not constant. It 'pulses' with a degree of regularity. This structure is previously unreported.

Figure 9 shows similar 'pulsing' in another porcine EKG signal. However, the structure is so pronounced that high energy, high frequency, intermittent components can be observed. These components have an occurrence frequency of the order of the original sinus rhythm: approximately 1.7Hz.

Figure 10a is a human EKG signal segment containing a shock event. Figure 10b is the corresponding wavelet scalogram. It is apparent from the scalogram of Figure 10b that both high frequency spiking and an intermittent high-energy region are present in the vicinity of 10 Hz and also above 10Hz.

The high frequency spiking is unique to the method of the present invention and is not visible using conventional Fourier techniques. The rich structure made visible within the EKG by the wavelet transform method is evident in the scalogram.

It is clearly seen from the Figures that applying the wavelet transform to an EKG signal of VF demonstrates that this signal is a rich source of valuable information. That is, it produces a display showing real time visualisation of the distribution of energies and coherent structures within the signal for use by a clinician in the selection of treatment strategies.

Using this method of analysis it is feasible to obtain real-time visual display of the EKG frequency characteristics in the wavelet domain during resuscitation. The scalogram produced provides information about the myocardium that is not available from a standard single channel surface EKG.

The wavelet scalogram decomposition can be displayed as a real time scrolling window, as shown in Figure 9. This window is useful as an aid for clinical decision making. It can be used as a stand-alone tool, or as basis for on-line statistical analysis of the current state of a heart.

To produce the window, a MATLAB TM R11 application is used. Each EKG sample taken results in the updating of a FIFO (First In First Out) buffer, and the EKG plot of Figure 9a. The scalogram of Figure 9b is then shifted

to the right and clipped before the 'missing' new right hand data is calculated, using conventional matrix algebra, and filled.

This results in the two scrolling windows of Figure 9. The exponential ramp in the bottom right corner shows the compact support of the wavelet utilised at the given scale.

Higher resolution scalograms are achieved through implementation on higher specification machines, purpose built hardware, or application specific software with coding using a lower level programming language, such as C++.

CPR produces artefacts in the EKG signal. Additionally, this method delivers information the value of which is not degraded once the CPR artefacts are filtered from the EKG signal.

From examination of the *scalograms* shown in Figures 6g, 7a and 7b it can be seen that the VF signature and the signature of the CPR artefacts occupy distinct areas of the scalogram, which permits their separation.

Known techniques such as the Modulus maxima method are now available to reduce the non-zero data points in the wavelet scalogram. This method reduces the topography of the scalogram surface to a series of ridges, thereby

considerably reducing the amount of data required to represent the signal in the wavelet space.

The modulus maxima obtained from a bandlimited signal with a wavelet of finite compact support in the frequency domain defines a complete and stable signal representation.

In this method, temporal filtering of the original EKG signal to disassociate the CPR signature from the heart signal can either be done directly, using the wavelet *energy scalograms*, or indirectly through modulus maxima techniques. This allows the heart to be monitored without necessitating cessation of CPR to allow rhythm recognition.

Further to the above, the method may also be applied to patients suffering form atrial fibrillation (AF) as a means of disassociating the prevalent QRS and T waves from the remainder of the signal.

Wavelet decomposition of the ECG signal is performed using an appropriate wavelet function. The modulus maxima technique is used to encapsulate the scalogram information in a series of ridges. Filtering of the signal is then undertaken using the modulus maxima information and through reconstruction the clinically useful information is isolated from the signal .

Specifically, Figure 15a shows the wavelet transform decomposition of a 2 second segment of ECG taken from a patient with atrial fibrillation. Below the ECG trace

is a wavelet scalogram plot. The corresponding modulus maxima of the scalogram is plotted below the scalogram.

For example, Figure 15d contains a 7 second segment of ECG exhibiting AF. The signal has been partitioned using a modulus maxima ridge following algorithm. The modulus maxima ridges have been separated into large and small scale features by thresholding the signal at a predetermined wavelet scale. A blow up of part of the signal is given in the lower three plots in the figure: Figures 15g, 15h and 15i. The middle of these plots contains the partitioned signal with the QRS complex and T wave filtered out revealing regular, coherent features that appear at a frequency of approximately 400 beats per minute, typical of AF. The lower plot contains the partition with the filtered out QRS and T waves. Although, a relatively simple modulus maxima technique was used in this pilot study whereby the modulus maxima lines were simple partitioned into two subsets, the ability of the technique to separate the signal into QRS and T waves and underlying atrial activity is evident from the results. It is known that the decay in amplitude of a modulus maxima corresponding to a signal feature can be a function of the scale of the wavelet. It is possible to use this property to separate the ridge coefficients into a noisy and coherent part. In this way, further differentiation of the modulus maxima information can be implemented within a more sophisticated algorithm. This will facilitate the further separation of background noise, QRS and T waves, and atrial activity.

This method thus facilitates useful interpretation of previously unintelligible EKG signals.

In patients presenting with uncoordinated rapid electric activity of the ventricle of heart, known as ventricular fibrillation (VF), there is no effective pulse and myocardial blood flow ceases. Even the institution of optimal cardio-pulmonary resuscitation (CPR) of the patient does not achieve more than 30% of the normal cardiac output. Ischaemia during cardiac arrest leads to a rapid depletion of myocardial high-energy phosphates, deterioration of transmembrane potentials, and disruption of intracellular calcium balance. Paradoxically, the myocardium in VF has supranormal metabolic demands. For this reason resuscitation attempts become less likely to succeed with the passage of time, and electrical defibrillating shocks increasingly result in asystole or EMD.

After prolonged cardiac arrest, the use of pharmacological measures or CPR before attempting defibrillation may increase the chances of successful resuscitation. This invention provides a robust and reliable method of analysis of the state of the myocardium in VF that prevents attempts to defibrillate at times that are unlikely to be successful, or even harmful to the heart. This method also provides an indication of the best way in which to optimise the metabolic state of the heart prior to counter-shock.

The method includes steps to establish a standard against which to evaluate collected data in a particular incidence.

The method further employs use of measurable signal characteristics derived from the position and amplitude of features in the *scalogram* to estimate both the condition of the myocardium, and downtime of the subject while in VF.

The method thus provides for optimal treatment of the heart in VF, so fulfilling specific patient needs, by therapeutic intervention, if appropriate.

An energy scalogram such as that shown in Figure 7 displays three distinct bands, labelled A, B, C. It is possible to derive quantifiable measures using correlations between the location and energy content of the bands.

Band A of Figure 7b represents the dominant energy band seen in the *scalogram* of Figure 7a, and corresponds to the tachycardic beating of VF. However the *scalogram* is much more informative in that it also shows, as bands B and C, the behaviour of other frequency components of the signal which were previously unreported.

Figure 7a shows a 2D *energy scalogram*. It includes the first 5 minute period of VF, followed by a 2.5 minute period of CPR. The onset of CPR is clearly identified by the distinct horizontal dark band in the lower right

quadrant of the Figure. Over the first 5 minute period, three bands, labelled A, B, C, can be clearly seen in the scalograms. These bands correspond to the ridges of Figures 6d to g. The increase in the frequency components of these three bands after the onset of CPR is evident in the plot. Bands B and C follow trajectories similar to each other in the *scalogram*, reducing in frequency over time. Band A, however, moves independently of the other two. Initially Band A increases, then it decreases to a local minimum value at approximately 70s. Between 70 and 160s it increases relative to Bands B and C. Finally, it decreases until the start of CPR after 300s. The same pattern was present in all 32 pig EKG traces of the experiment.

Obvious increases in the passband frequency of all three bands are observed in the *scalogram* after the onset of CPR. For some of the signals studied this increase in band C is masked by the dominant CPR band, and thus cannot be seen in the *scalogram*.

Figure 7b provides a schematic diagram of the salient features contained within the scalogram plots, where t0 is immediately after the onset of VF; t2 is the start of CPR; and t3 is the end of the analysis. Figure 7c shows the relative proportion of energy contained in the scalogram in the 5 to 12 Hz region through time. There is an obvious decay in the relative energy associated with this region which is associated with the breakdown of co-ordinated activity in the heart.

The steps of the method of the present invention described above establish that during the course of VF there is a reduction in the proportion of energy within the dominant frequency band indicated in Figure 7c. This dominant frequency band, Band A in Figure 7a, is demonstrated to be approximately 10 Hz for pig VF.

The energy within this band changes rapidly. This is illustrated by the 'pulses' in Figures 8,9,10.

The Figures 6,7,8,9,10 show that applying the wavelet transform to an EKG signal of VF demonstrates that this signal is a rich source of valuable information.

The underlying hypothesis of the method of the present invention is that the scalogram associated with an EKG correlates to the state of the myocardium as it decays subsequent to the onset of VF.

The method uses the information contained in the energy scalogram associated with an EKG to predict the likely success of clinical intervention, namely shocking.

It is therefore possible to develop a wavelet transform based tool for the prediction of shock outcome during ventricular fibrillation by:

1. collecting and collating data from sets of archived EKGs recorded from humans in VF where attempts to resuscitate by shocking were made; and

2. developing a classifier for reference purposes.

Figure 11 is a classification of the shock outcome in either asystole or a rhythmic response using a relatively simple statistical analysis. The experiment yielding the results to compile these Figures involved use of the lead II outputs of standard three lead EKGs of 120 patients in VF. Each trace is of three second duration sampled at 100 Hz. Of these patients, 60 returned to sinus rhythm while the other 60 deteriorated to asystole, post shock.

Each trace was decomposed into an associated wavelet transform from which its energy scalogram was generated. The volume under this surface was then normalised to render the results independent of signal amplitude, but instead the result of the relative wavelet constituents of the signals. The log of the mean values at each dilation (band centre frequency) for each was then recorded. Figures 11a and 11b show the distribution of energies in a lower frequency band (1.9 Hz) and at the 9.3 Hz band. Clearly, through visual inspection, it is apparent that the proportion of energies around the 10 Hz band is higher for successful defibrillation attempts.

The method then extends to apply neural techniques to analysis of wavelet pre-processed EKG signals.

A pilot study conducted to determine the feasibility of using artificial neural techniques to provide a tool to predict the outcome of defibrillation during VF used eight human EKG trace segments containing shock events.

In these cases, the result of shocking was unequivocal - four patients returned to VF, and four experienced return of spontaneous circulation (ROSC).

The traces were transformed using the Morlet wavelet, and energy scalograms containing thirty frequency levels were produced. This was then split into eight overlapping sections as shown in Figure 12a, each of 200 points (2/3 seconds duration). These 200 location points were subsampled down to 50 to give eight scalograms for each trace of 50 x 30 elements. The volume under the energy scalograms were normalised and the patterns fed into a 'winner take all' Kohonen network with two output units and built in *conscience* (to avoid local minima). That is, the network was asked to group the 64 input patterns into two classes. All but ten outputs were collectively classified correctly giving a mean pattern error of 0.156 (against 0.5 average pattern error expected from random inputs).

Since this is a vector quantisation method (VQM) it was possible to identify how the network differentiates the patterns through inspection of its connective weights. The weights from each location position across all scales in the network are approximately the same, which means that there are no markers with which to synchronise the different pre-processed traces. This confirms that this neural network is too simple for this purpose. That is the network is not equipped to 'consider' the relative phase of each input pattern.

Figure 12b shows the weights for the 'success' (ROSC) and 'failure' (VF) to the output units from the first two time slices across all scales. The weights indicate the classes are differentiated by the proportion of energy in the lower scales, which can be seen when compared with Figure 11.

Although the above described method indicates the slight drop in the dominant frequency expected, the drop is very marginal which leads to the conclusion of the lack of competence of previously proposed methods as a defibrillation success predictor.

In summary, a library of human ECG data containing data sets of human VF with attempts to resuscitate by shocking is used as a database. This database is extended to include data sets containing various methods of shocking including, for example, biphasic shocking. The biphasic shock waveform has resulted in an increased proportion of successful defibrillation attempts and is set to become the standard treatment for cases of VF.

In one example, the recognised outcomes are defined by trace components of the post-shock window lasting until next shock (if present). If the ratio of the given rhythm exceeds 10% of the total window length the rhythms are prioritised according to the sequence:

Class	**Rhythm**	**Ratio**
1	Pulse (SVR)	+10%

2	No pulse (EMD)	+10%
3	Isoelectric (Asystole)	+10%
4	VF	+10%

Class 5 is the class of VF preceding shocks where VF re-establishes itself within 5 seconds following the shock (i.e. no change). The VF in all the other classes were non-VF in this period.

Wavelet analysis of this information in accordance with the method of the invention is then performed to:

construct a wavelet visualisation of the signal - usually by plotting wavelet energy surfaces against the location parameter *b* and the inverse of the dilation parameter *a*;

provide measurable characteristics of the signal for estimation of downtime of the patient;

provide measurable characteristics of the signal for determining the health of the heart post CPR; and

to construct energy scalogram devised for the method - which uses the energy density function and the reciprocal of the wavelet *a* scale for use as a predictor tool.

As described above it is possible to use artificial neural network based techniques to develop such an indication of the state of myocardium. In the

alternative, it is possible to classify the wavelet scalogram through multilayered feedforward network types.

The method may include the development of a modulus maxima algorithm tool for the preprocessing of ECG prior to its input into a neural network classifier.

Using this technique improves network performance whether this data is further encoded, or presented as a whole, larger, sparse matrix as a pattern in the input space.

This method therefore utilises the generalisation properties of a feed forward multi-layer network to predict the likelihood of defibrillation success from the wavelet transform of the EKG traces. This multi-layer network with its relatively simple dynamics, when combined with wavelet pre-processing, has proved itself a useful tool as a universal approximator.

The classes of multi-layer network types of use in this method are:

- Multi-layered feed forward (MLFF) neural networks with back propagation training and monotonic activation functions; and
- Radial Basis Neural Networks (RBNN) as have previously been successfully applied to the denoising of medical Doppler ultrasound signals with wavelet preprocessing.

As described above, the method involves the decomposition of EKG signals into a complete basis set defined by the wavelet shape and other parameters by salient basis functions of a different basis set, converged upon through regression techniques (sigmoid in the case of multilayer neural networks, Radial basis etc).

These regression techniques can also be used to construct a wavelet basis function set directly.

Methodologies for restricting the search space of the wavelet basis functions considered are known. Whilst this wavelet network has been shown to be effective for chaotic time series prediction, its implementation involves the use of wavelet *frames* of a decimated, dyadic, construction. The method of the present invention may employ continuous wavelet networks spanning a redundant wavelet *basis* which, although computationally more expensive, overcomes the time invariance constraint and the limited size of input space associated with use of wavelet frames.

The method may use conventional gradient decent methods to produce a single layer wavelet classifier.

These wavelet networks may be further employed as part of a multilayer system as a non-parameterised estimate of the original trace for input to further hidden layers.

The network type of choice for the automated prediction system of the method is selected on the basis of its sensitivity and selectivity in correctly classifying successful defibrillation outcomes in test set data, since this is most clinically useful.

Thus experimental comparison of the three techniques demonstrates the efficacy of the wavelet transform technique.

The nature of underlying atrial activity can also be determined from wavelet decomposition of the EKG signal. The wavelet function gives information regarding the amplitude and, where appropriate, phase of the transformed signal. It is known that pressure readings taken from the aorta correlate to forms of atrial activity within the heart. Areas of localised high energy contained within the scalogram can be demonstrated to correlate with these pressure readings. This experimental result is extrapolated to mean that areas of localised high energy contained within the scalogram correlate with forms of atrial activity within the heart.

Figure 13a shows the aorta pressure, Figure 13b the EKG trace, for the same time period as Figure 13a, and Figure 13c shows the scalogram for the EKG of Figure 13b. It is apparent that there is an increase in energy in the system during an atrial pulse, indicated by the dark blotches occurring in the scalogram at an f_{bpc} of around 10 Hz. There is a frequency component between 1 and 2 Hz. As shown in Figure 13d, which

highlights the phase of the scalogram between 1 and 2 Hz, it is apparent hat the lines of zero phase are in alignment with the atrial pulse.

In a further scalogram, shown in Figure 13e, produced by using the Mexican hat wavelet transform which is real and has better temporal resolution, but worse frequency resolution than the complex scalogram of Figure 13c, it is demonstrated that positive high amplitude components are shown at the same positions for scales of between 1 and 2 Hz, thus reinforcing the findings extrapolated from Figure 13c. That is as shown in Figure 13f, the lines of zero phase correlate with the pulse position.

The lines of zero phase within the 1.8Hz frequency band also align with regular peaks in the scalograms, as shown in Figures 14a, 14b & 14c. This links the presence of the 1.8 Hz band with the observed peaks at higher frequencies. This correlation between the 1.8 Hz band and the aorta pressure pulse suggests atrial activity is present.

In a further application of the method, means for identifying the optimum timing for application of the defibrillation shock can be extrapolated from the pulsing identified by the wavelet technique and shown in Figures 8, 9, 10, and 14, by comparison with traces of attempts at defibrillation which initially fail but are subsequently successful.

Thus, any data sets, in the above, that correspond to multiple shocking of the same patient, where defibrillation has been repeatedly attempted are considered separately since these traces hold important information.

The pilot study detailed above used Morlet wavelet based energy scalogram decomposition of signal segments immediately prior to shocking. A full parametric wavelet study of the method determines the optimum method.

The method includes the development of a classifier using the wavelet transform analysis.

Various types of neural network classifier are achievable using this method.

The linkage of shock timing to the phase information of wavelet components allows for increased defibrillation success and reduced shock energies. The wavelet-derived information can also be employed to predict the likelihood of shock success, preventing futile or harmful defibrillation attempts, and providing a predictor of an optimal resuscitation strategy or strategies.

This method demonstrates the utility of the wavelet transform as a new method of EKG signal analysis during VF. It provides a robust, real-time solution to the

problem of useful monitoring of the myocardium during resuscitation.

When compared with conventional statistical methods, such as fast Fourier transforms, it is seen that the temporal resolution of the wavelet technique gives a scalogram which better describes the non-stationary, intermittent, nature of the EKG trace to be analysed, and gives a method of greater predictive effectiveness than is already known. The effectiveness criteria for the networks of the method of the present invention are based upon their sensitivity and selectivity in correctly classifying successful defibrillation outcomes from test data sets.

Although this description refers to wavelet transform analysis, this term is to be construed to include matching pursuit algorithms and similar analysis techniques.

Modifications and improvements can be made to the above without departing from the scope of the invention.

CLAIMS

1. A method of decomposition of waveforms in a cardiac signal using wavelet transform analysis.

2. A method as claimed in Claim 1 comprising the step of employing discretized wavelet transform analysis to process the said waveform.

3. A method as claimed in Claim 1 comprising the step of employing discretized continuous wavelet transform analysis to process the cardiac waveform.

4. A method as claimed in any preceding claim comprising the steps of deriving the wavelet energy surfaces of an electrocardiogram (EKG) signal; and plotting said wavelet energy surfaces against a location parameter b, and a scale parameter.

5. A method as claimed in Claim 4 wherein said scale parameter is dilation a.

6. A method as claimed in Claim 4 wherein said scale parameter is band pass frequency f_{bpc}.

7. A method as claimed in any preceding claim comprising the initial steps of connecting electrodes to a presenting patient; and sampling the analogue input signals recorded to derive the cardiac signal.

8. A method as claimed in any preceding claim including visually displaying the cardiac signal.

9. A method as claimed in any preceding claim including visually displaying the distribution of energies within the cardiac signal.

10. A method as claimed in any preceding claim including visually displaying coherent structures within the cardiac signal.

11. A method as claimed in any preceding claim including visually displaying the signal in real-time for clinical use.

12. A method as claimed in any preceding claim comprising the step of constructing a contour plot to display the decomposed waveform obtained.

13. A method as claimed in any preceding claim comprising the step of constructing a surface plot to display the decomposed waveform obtained.

14. A method as claimed in any preceding claim comprising the step of constructing a 2D or a 3D energy scalogram to display the decomposed waveform obtained.

15. A method as claimed in any preceding claim including the step of disassociating the component features of the temporal trace of a recorded EKG.

16. A method for the analysis of an EKG of a heart in ventricular fibrillation including the method as claimed in any preceding claim.

17. A method for the analysis of an EKG of a heart in ventricular fibrillation after the commencement of cardio-pulmonary resuscitation (CPR) including the method as claimed in any of Claims 1 to 15.

18. A method as claimed in Claim 17 including the step of temporal filtering of the EKG signal of a heart that is subject to CPR to disassociate the CPR signal from the heart signal.

19. A method as claimed in Claim 17 or Claim 18 using wavelet *energy scalograms*.

20. A method as claimed in Claim 17 or Claim 18 using ridge following techniques

21. A method as claimed in Claim 20 wherein said ridge following techniques are modulus maxima techniques.

22. A method for the estimation of the health of a heart in VF including the method of any of Claims 1 to 15 to provide measurable characteristics.

23. A method as claimed in Claim 22 wherein said measurable characteristics are used to provide an estimate of the time elapsed since the onset of a cardiac incident.

24. A method as claimed in Claim 22 wherein said measurable characteristics are used to provide an estimate of the health of a heart after commencement of CPR.

25. A method as claimed in any of Claims 22 to 24 wherein said measurable characteristics are used to predict the outcome of a given therapeutic intervention.

26. A method as claimed in any of Claims 22 to 25 wherein said measurable characteristics are used to provide a guide for the optimal timing of defibrillation of a heart in VF.

27. A method for the analysis of an EKG of a heart in atrial fibrillation including the method as claimed in any of Claims 1 to 14.

28. A method as claimed in Claim 27 including the step of partitioning the signal to provide separate traces of QRS and T waves, and/or atrial activity and/or background noise.

29. A method as claimed in any preceding claim including the step of constructing a damage index for reference purposes.

30. A method as claimed in Claim 29 wherein construction of said index includes the step of developing network classifier from a library of recorded data.

31. A method as claimed in Claim 30 wherein said network classifier developed is a neural network.

32. A method as claimed in any of Claims 29 to 31 wherein said network classifier developed is a wavelet network classifier.

33. A method of decomposition of cardiac waveforms using matching pursuit algorithms.

34. Apparatus for decomposition of waveforms in a cardiac signal, said apparatus comprising wavelet transform analysis means.

35. Apparatus as claimed in Claim 34 including means to display the distribution of energies within a waveform.

36. Apparatus as claimed in Claim 34 or Claim 35 including a monitor adapted to display decomposed waveforms.

37. Apparatus as claimed any of Claims 34 to 36 adapted for inclusion in an EKG apparatus.

38. Defibrillation means adapted to operate in response to a signal generated by comparison of an EKG trace with decomposed waveform obtained by the method of any of Claims 1 to 33.

39. A method as described in any of Claims 1 to 33 with reference to or as shown in the accompanying drawings.

40. Apparatus as described in any of Claims 34 to 38 with reference to or as shown in the accompanying drawings.

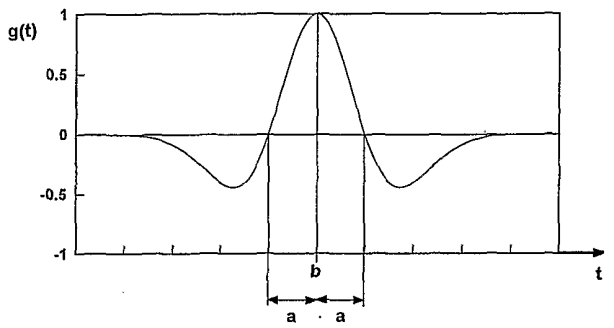

Figure 1(a)

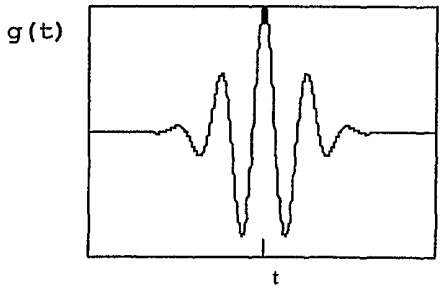

Figure 1(b)

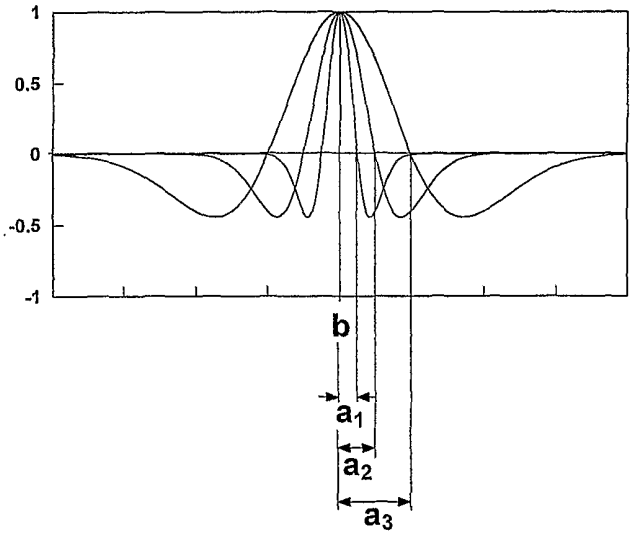

Figure 2(a)

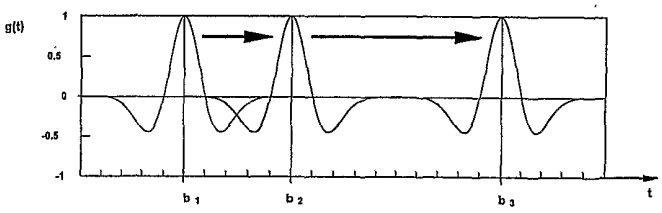

Figure 2(b)

Figure 3 (a)

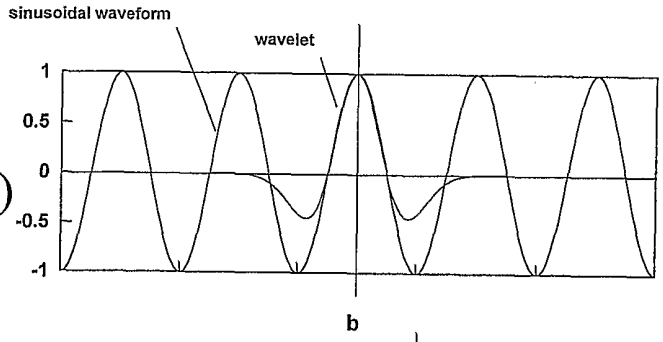

Figure 3 (b)

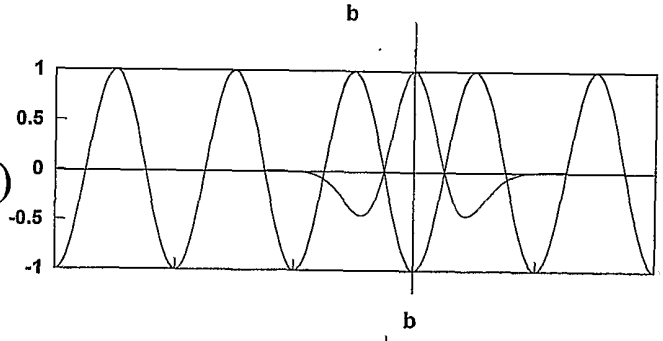

Figure 3 (c)

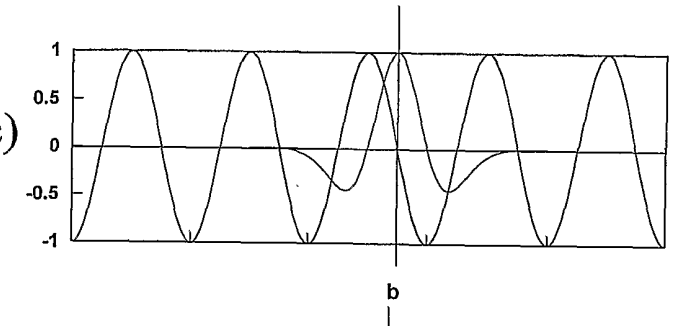

Figure 3 (d)

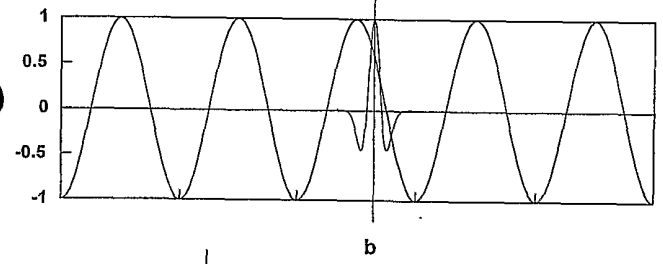

Figure 3 (e)

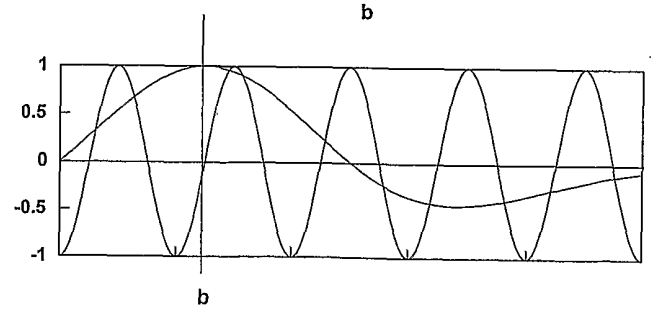

Figure 4 (a)

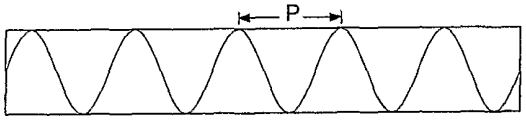

Figure 5 (a)

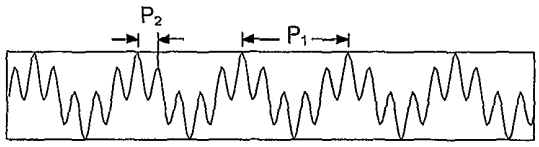

Figure 4 (b)

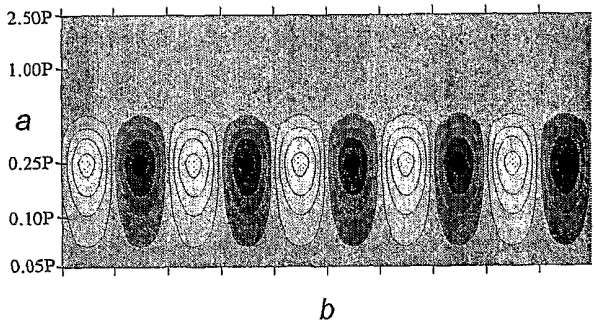

Figure 5 (b)

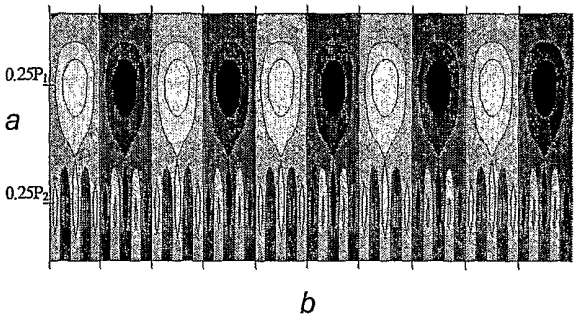

Figure 4 (c)

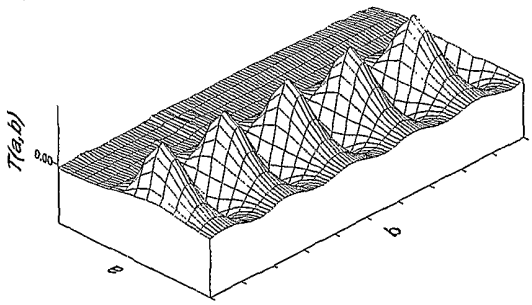

Figure 5 (c)

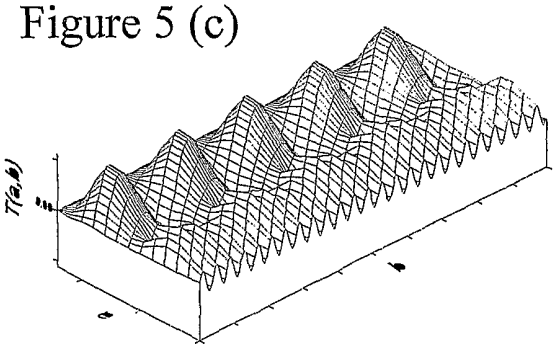

Figure 6 (a)

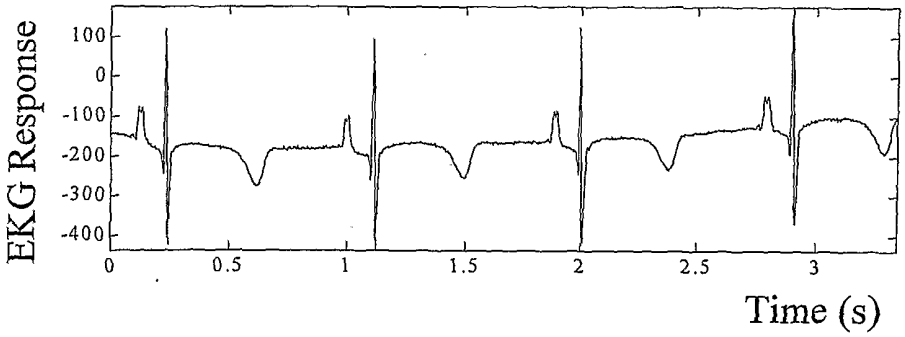

Figure 6 (b)

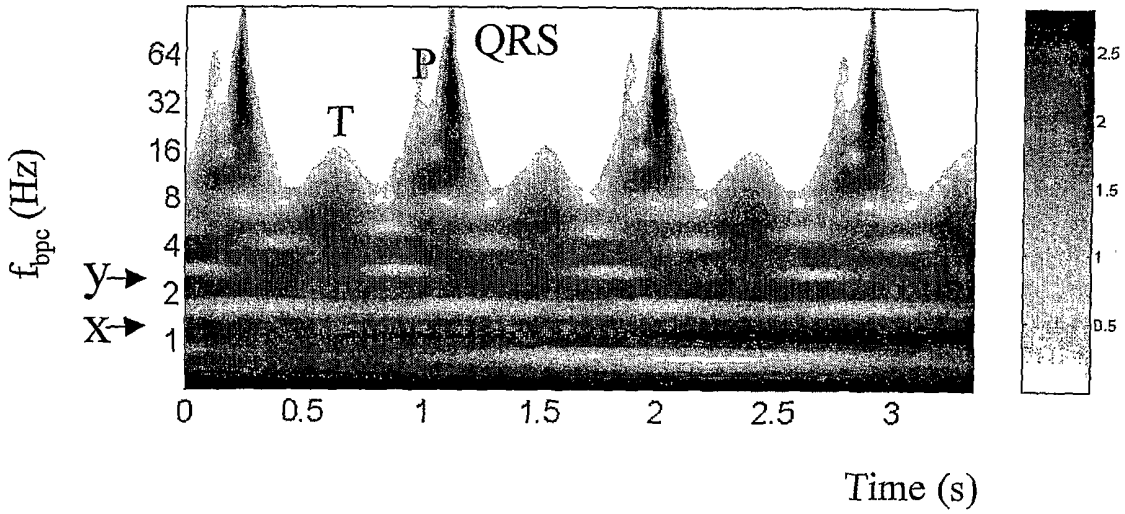

Figure 6 (c)

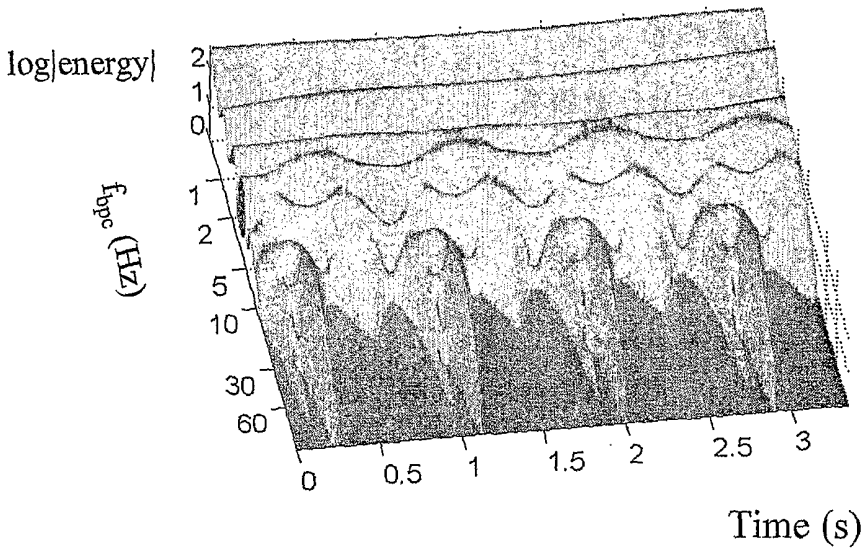

Figure 6 (d)

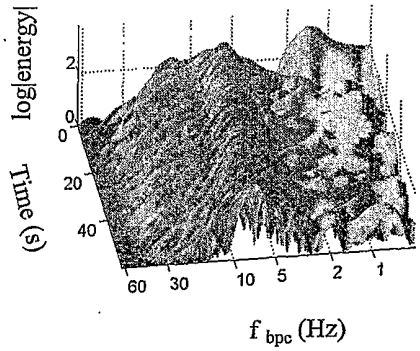

Figure 6 (e)

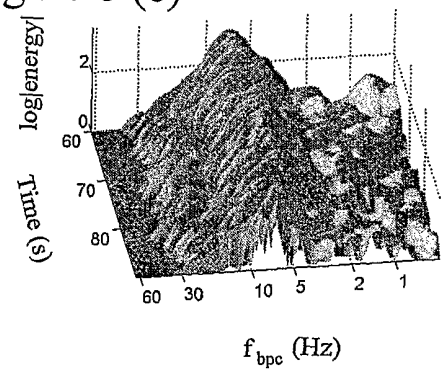

Figure 6 (f)

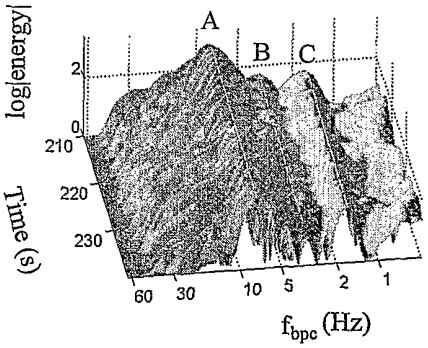

Figure 6 (g)

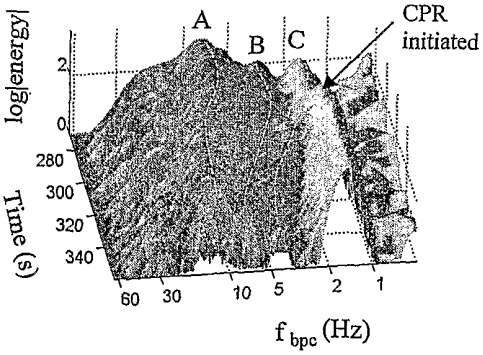

Figure 7 (a)

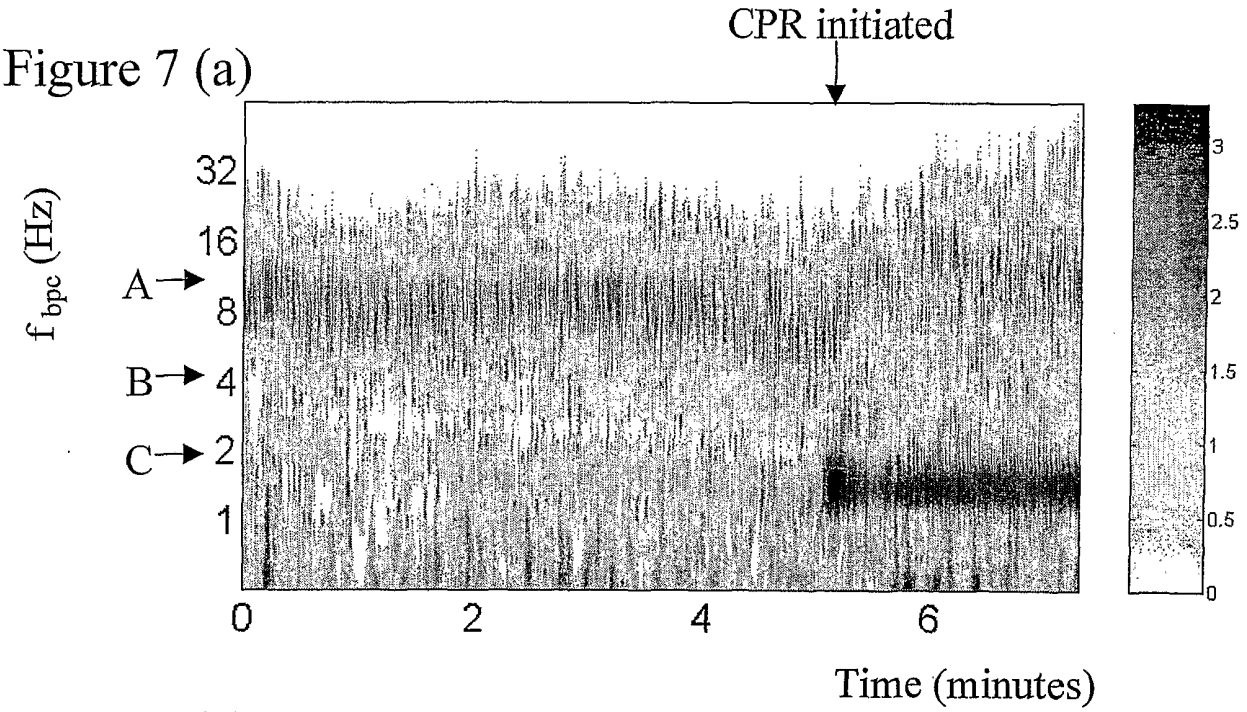

Figure 7 (b)

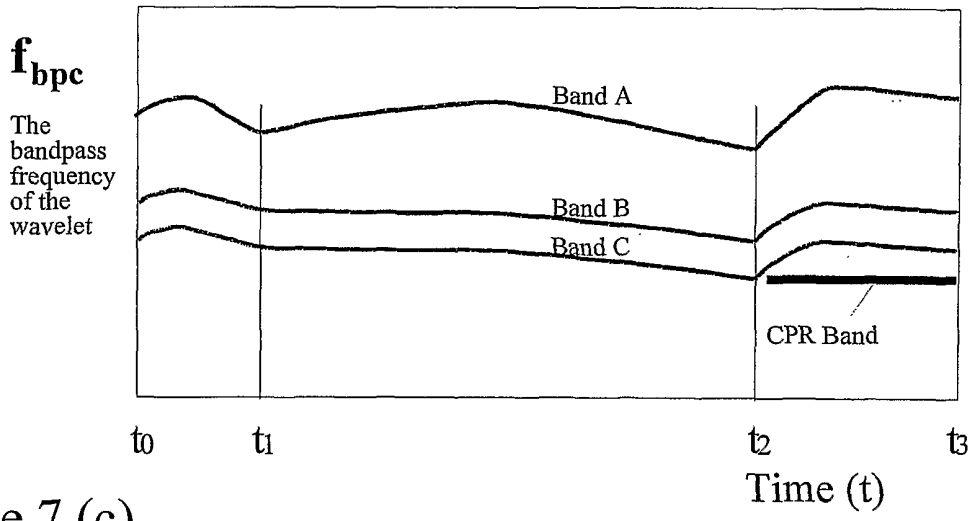

Figure 7 (c)

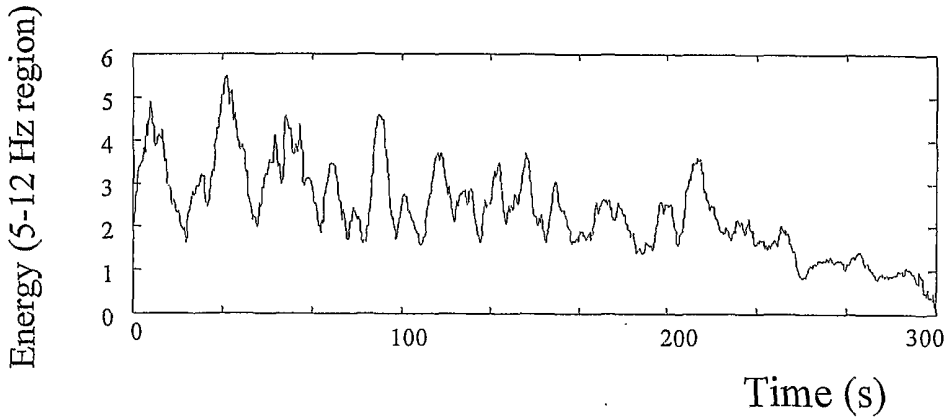

Figure 8 (a)

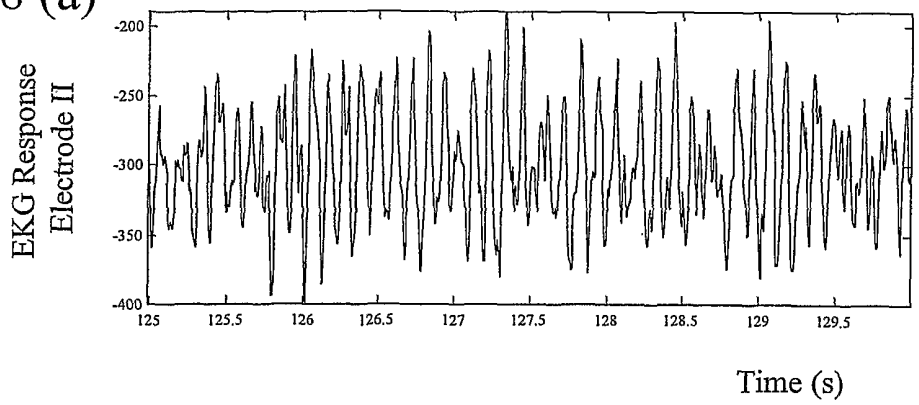

Figure 8 (b)

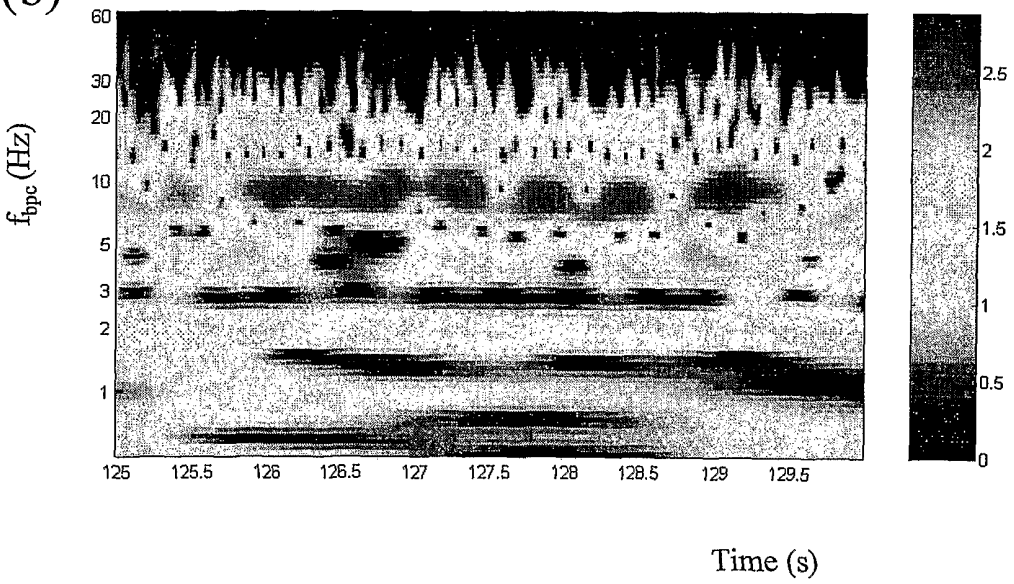

Figure 8 (c)

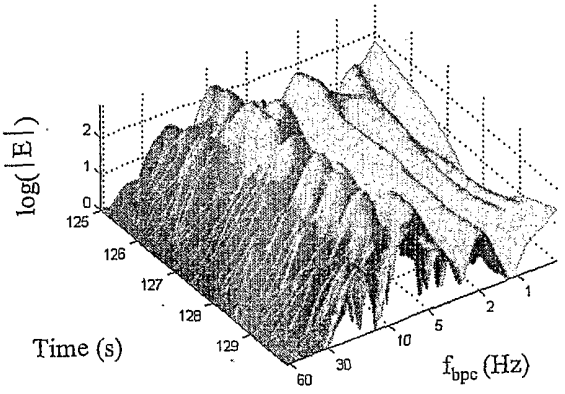

Figure 8 (d)

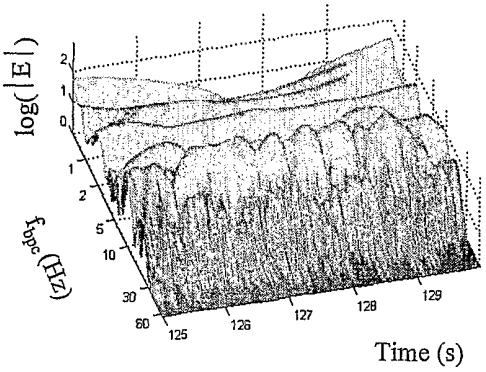

Figure 9

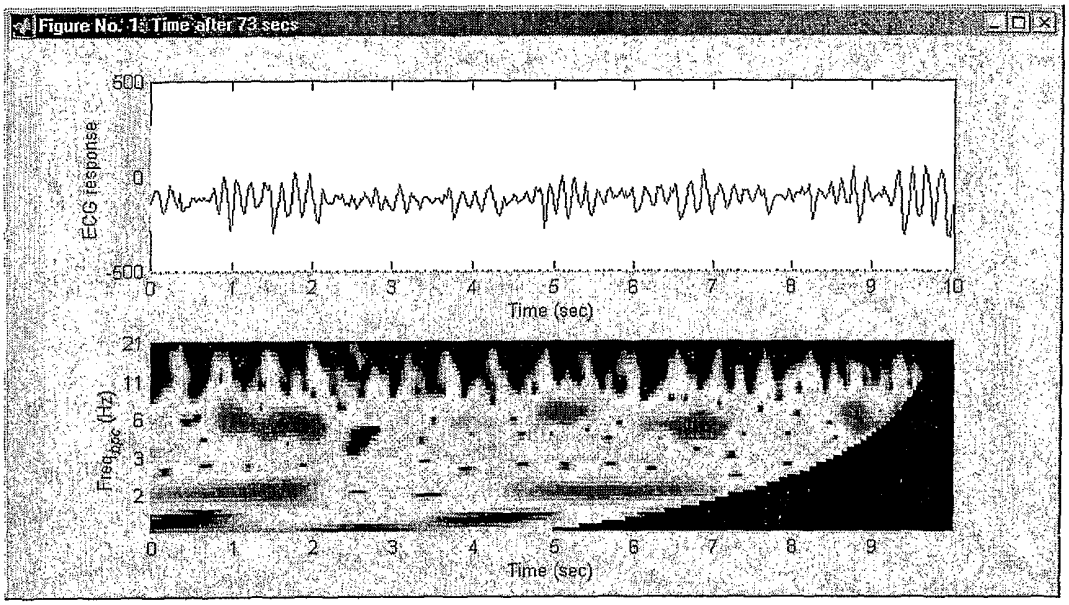

Figure 10 (a)

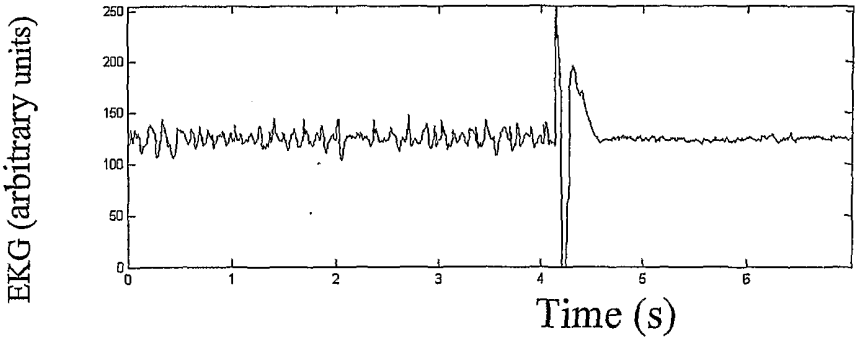

Figure 10 (b)

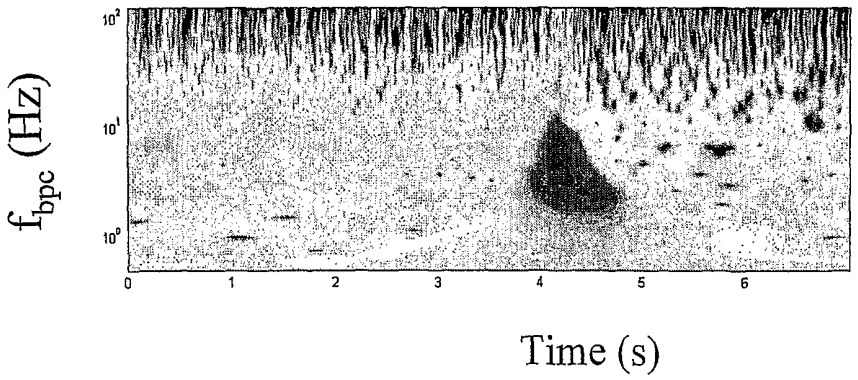

Figure 11 (a)

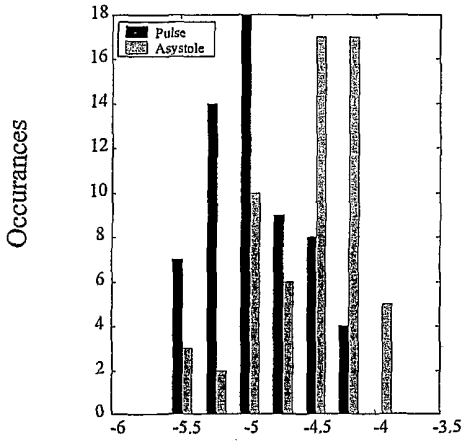

1.9 Hz

Figure 11 (b)

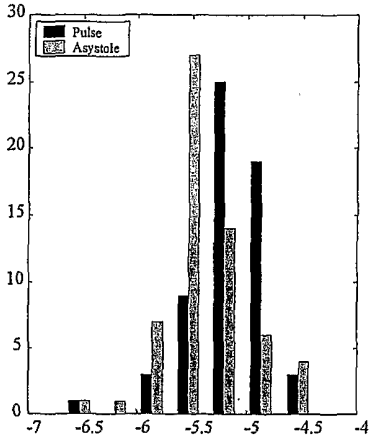

9.3 Hz

mean energy (log)

Figure 12 (a)

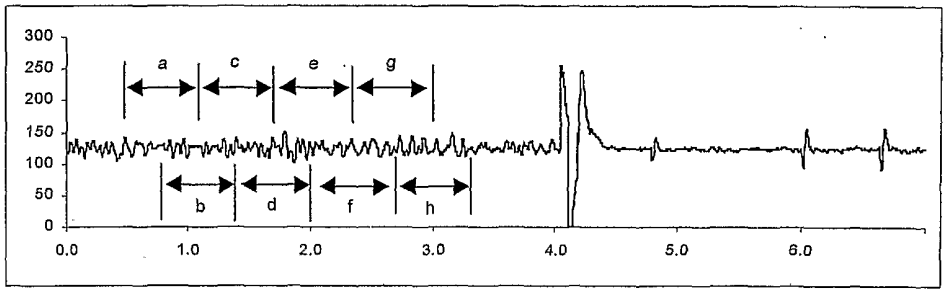

Weight value

Figure 12 (b)

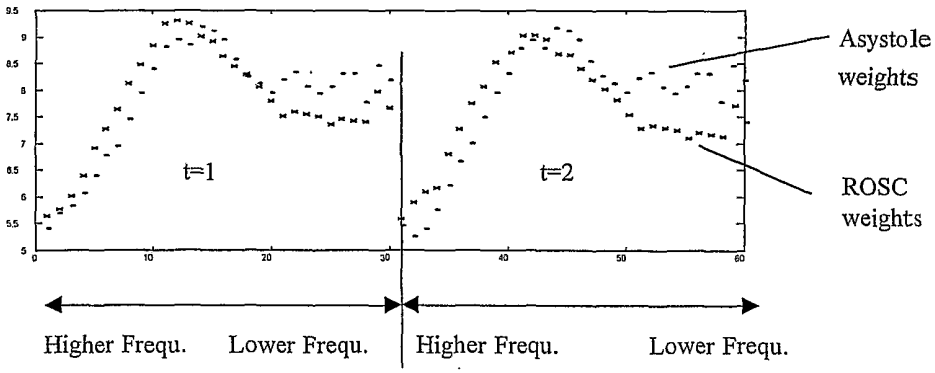

Figure 13 (a)

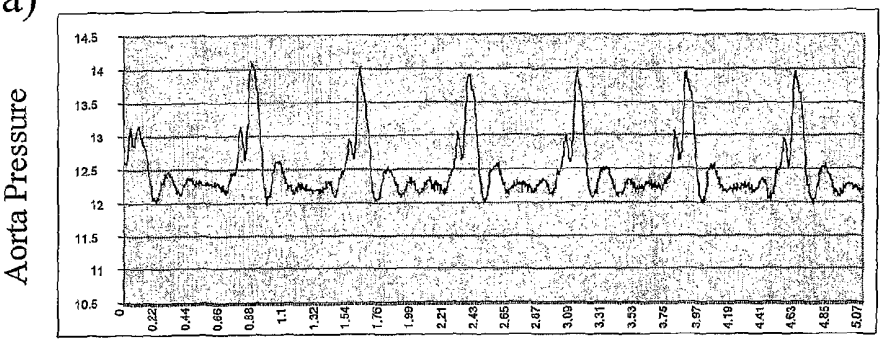

Figure 13 (b)

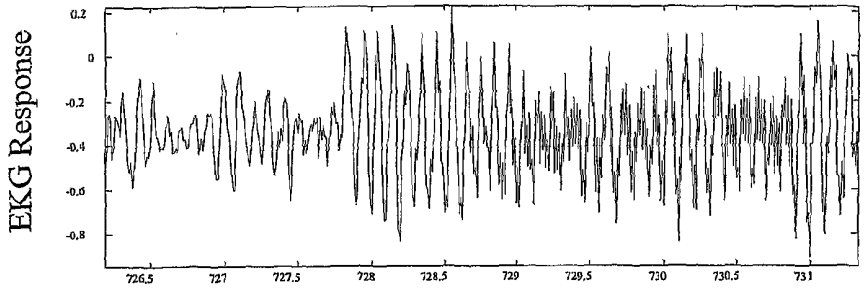

Figure 13 (c)

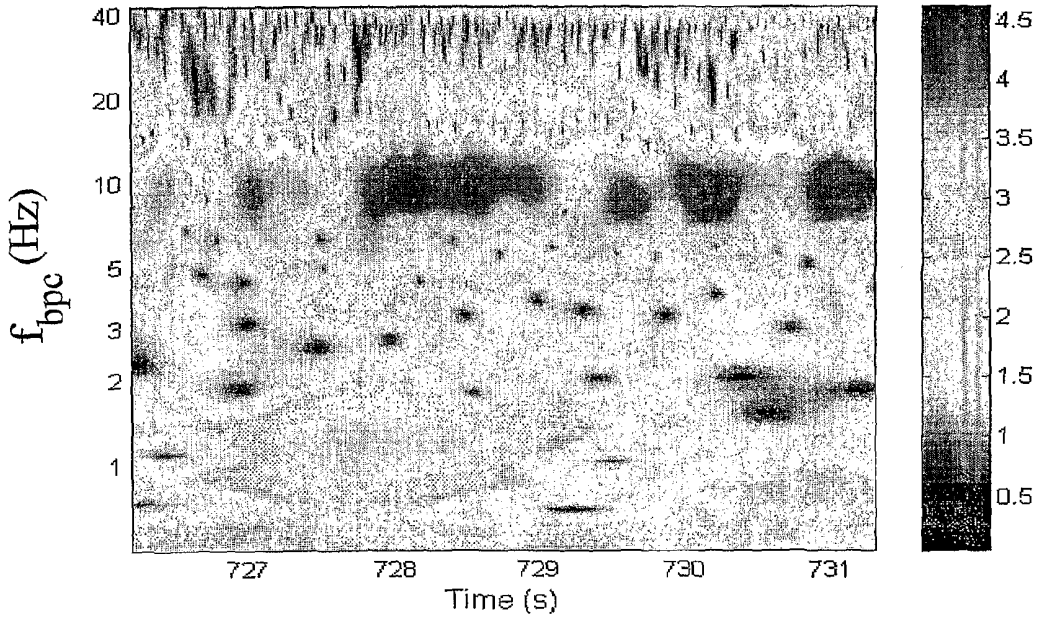

Figure 13 (d)

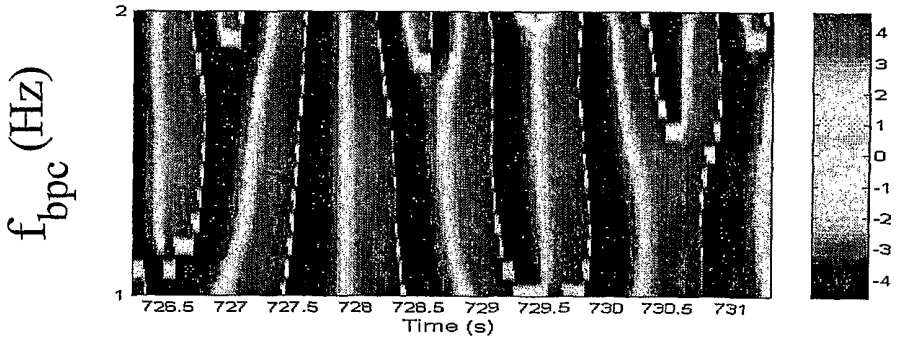

Figure 13 (e)

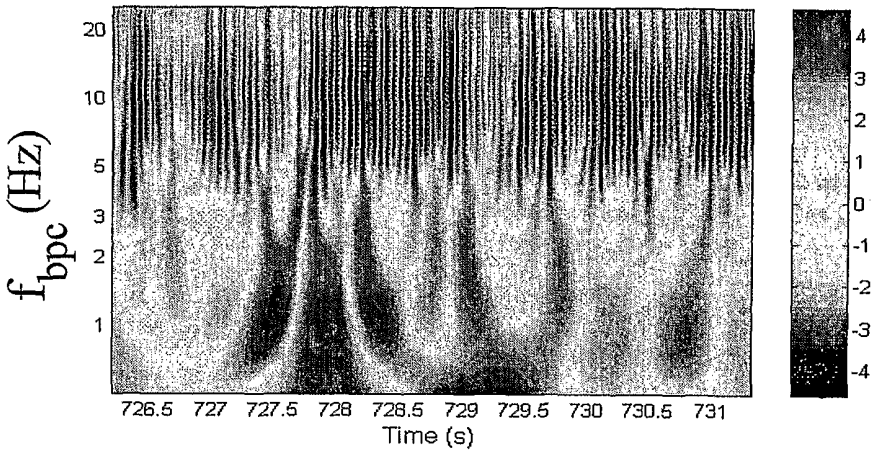

Figure 13 (f)

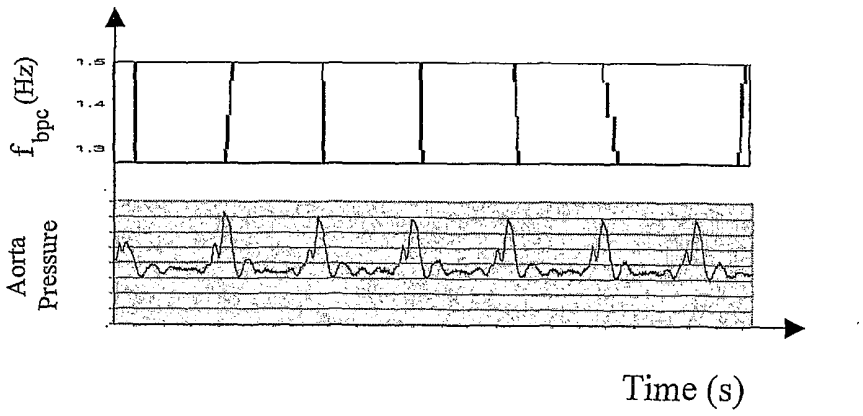

Figure 14 (a)

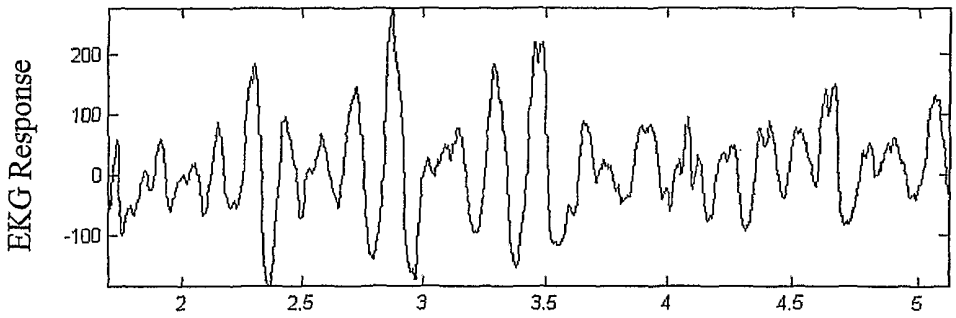

Figure 14 (b)

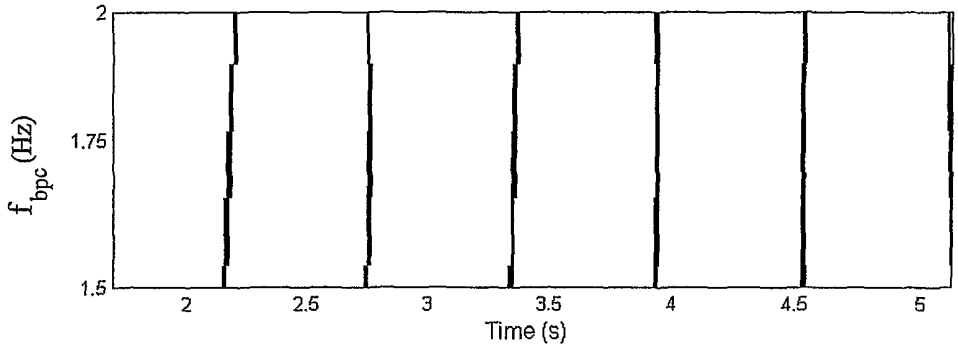

Figure 14 (c)

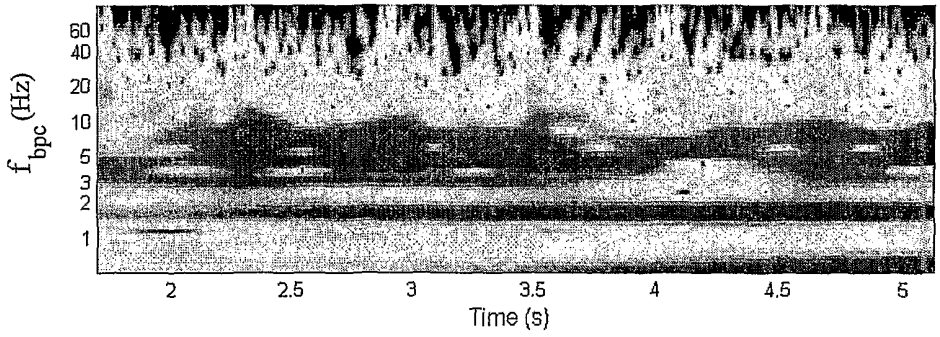

Figure 15 (a)

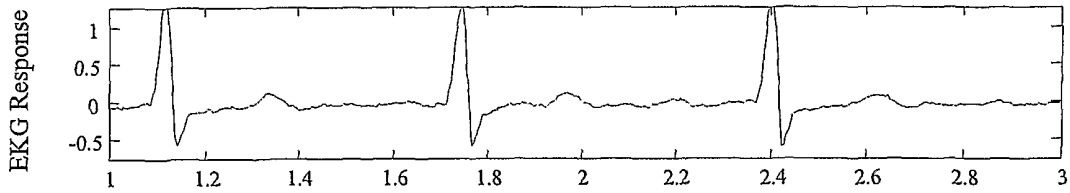

Figure 15 (b)

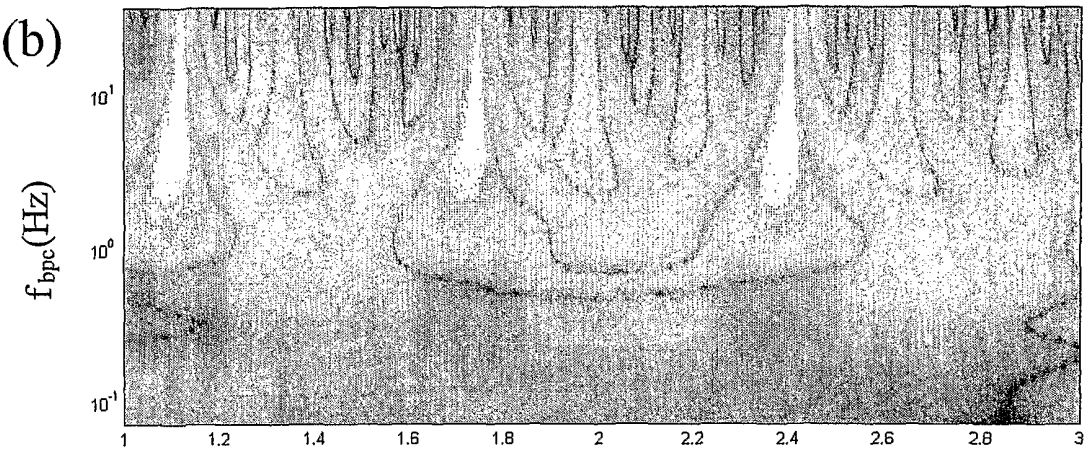

Figure 15 (c)

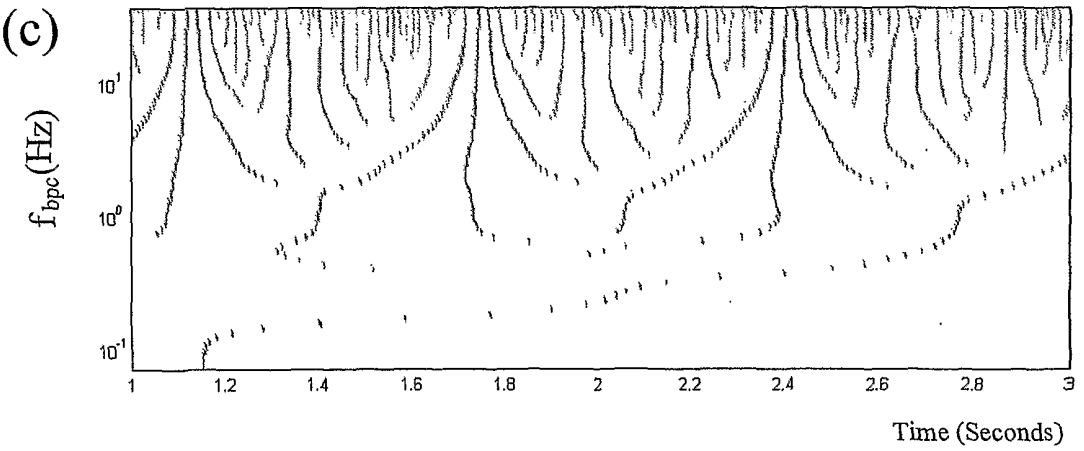

Figure 15 (d)

Figure 15 (e)

Figure 15 (f)

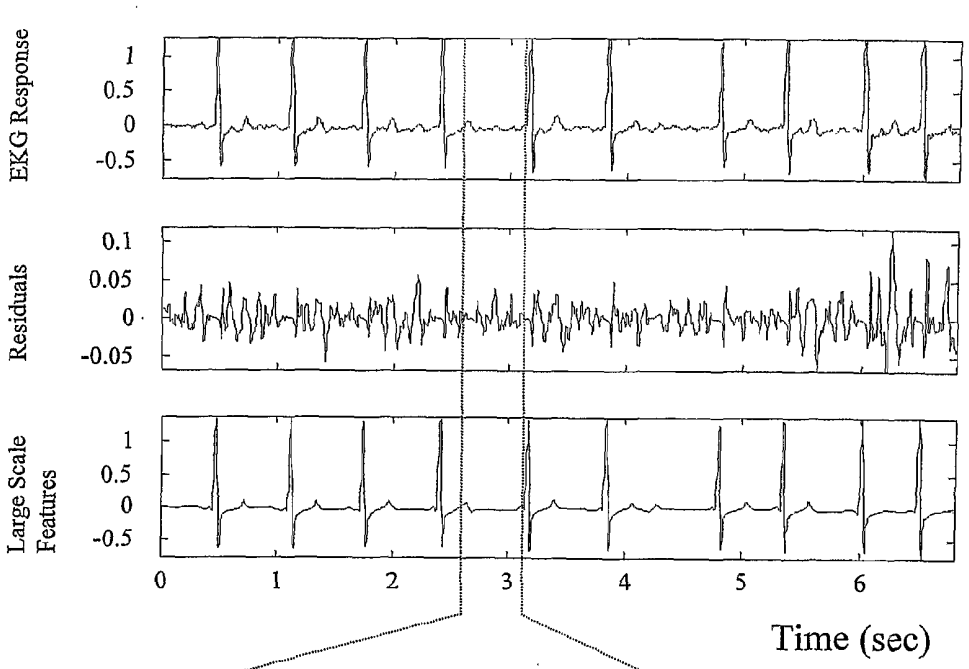

Figure 15 (g)

Figure 15 (h)

Figure 15 (i)

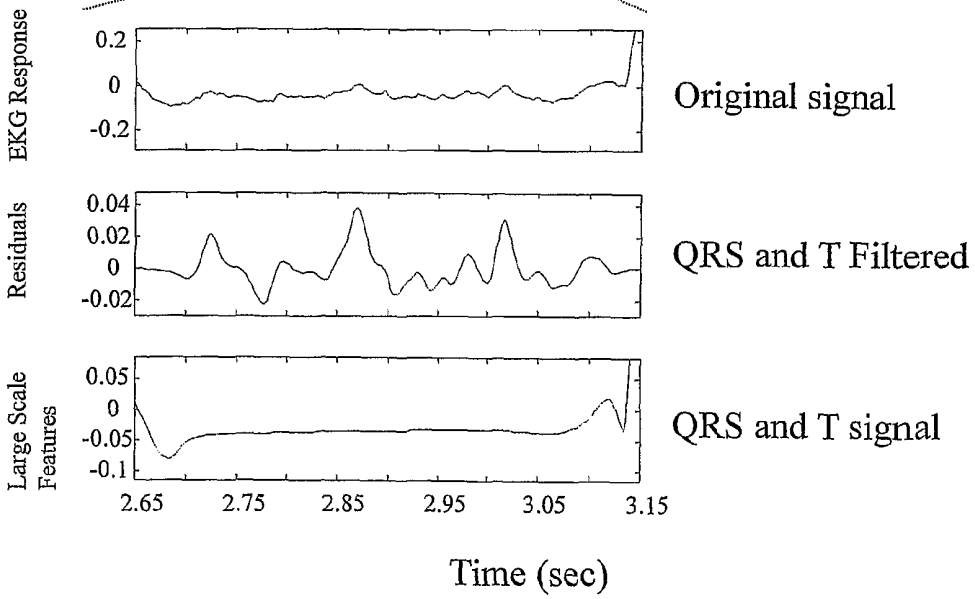

INTERNATIONAL SEARCH REPORT

International Application No
PCT/GB 00/01675

A. CLASSIFICATION OF SUBJECT MATTER
IPC 7 G06F17/00

According to International Patent Classification (IPC) or to both national classification and IPC

B. FIELDS SEARCHED

Minimum documentation searched (classification system followed by classification symbols)
IPC 7 G06F A61N

Documentation searched other than minimum documentation to the extent that such documents are included in the fields searched

Electronic data base consulted during the international search (name of data base and, where practical, search terms used)
EPO-Internal, WPI Data, PAJ, INSPEC

C. DOCUMENTS CONSIDERED TO BE RELEVANT

Category °	Citation of document, with indication, where appropriate, of the relevant passages	Relevant to claim No.
X A	WO 96 08992 A (SHOSHAN HERBERT Z ;UNIV RAMOT (IL); AKSELROD SOLANGE (IL); KESELBR) 28 March 1996 (1996-03-28) page 9, line 27 -page 11, line 9 page 13, line 29 -page 14, line 14 ---	1,2,7-9, 12-15, 34-37 3-5,10, 11,16
X A	US 5 439 483 A (DUONG-VAN MINH) 8 August 1995 (1995-08-08) column 4, line 36-49 --- -/--	1,2,7, 16,22,34 3,23, 25-27,38

[X] Further documents are listed in the continuation of box C.

[X] Patent family members are listed in annex.

° Special categories of cited documents :

"A" document defining the general state of the art which is not considered to be of particular relevance

"E" earlier document but published on or after the international filing date

"L" document which may throw doubts on priority claim(s) or which is cited to establish the publication date of another citation or other special reason (as specified)

"O" document referring to an oral disclosure, use, exhibition or other means

"P" document published prior to the international filing date but later than the priority date claimed

"T" later document published after the international filing date or priority date and not in conflict with the application but cited to understand the principle or theory underlying the invention

"X" document of particular relevance; the claimed invention cannot be considered novel or cannot be considered to involve an inventive step when the document is taken alone

"Y" document of particular relevance; the claimed invention cannot be considered to involve an inventive step when the document is combined with one or more other such documents, such combination being obvious to a person skilled in the art.

"&" document member of the same patent family

Date of the actual completion of the international search	Date of mailing of the international search report
13 September 2000	22. 12. 2000

Name and mailing address of the ISA	Authorized officer
European Patent Office, P.B. 5818 Patentlaan 2 NL - 2280 HV Rijswijk Tel. (+31-70) 340-2040, Tx. 31 651 epo nl, Fax: (+31-70) 340-3016	Grobmann, C

Form PCT/ISA/210 (second sheet) (July 1992)

INTERNATIONAL SEARCH REPORT

International Application No
PCT/GB 00/01675

C.(Continuation) DOCUMENTS CONSIDERED TO BE RELEVANT

Category °	Citation of document, with indication, where appropriate, of the relevant passages	Relevant to claim No.
X	DATABASE INSPEC [Online] INSTITUTE OF ELECTRICAL ENGINEERS, STEVENAGE, GB; 13 September 1998 (1998-09-13) MILLET-ROIG J; LOPEZ-SORIANO JJ; MOCHOLF A ET AL.: "Study of frequency and time domain parameters extracted by means of wavelet transform applied to ECG to distinguish between VF and other arrhythmias" XP002145546 abstract ---	1,2,16
X	CHEN J ET AL: "ECG DATA COMPRESSION BY USING WAVELET TRANSFORM" IEICE TRANSACTIONS ON INFORMATION AND SYSTEMS,JP,INSTITUTE OF ELECTRONICS INFORMATION AND COMM. ENG. TOKYO, vol. E76-D, no. 12, 1 December 1993 (1993-12-01), pages 1454-1461, XP000435570 ISSN: 0916-8532 abstract ---	1,2
X	DATABASE INSPEC [Online] INSTITUTE OF ELECTRICAL ENGINEERS, STEVENAGE, GB; 5 November 1996 (1996-11-05) GEVA A B: "Spatio-temporal matching pursuit (STOMP) for multiple source estimation of evoked potentials" XP002145547 abstract ---	33
X	SAVA H ET AL: "APPLICATION OF THE MATCHING PURSUIT METHOD FOR STRUCTURAL DECOMPOSITION AND AVERAGING OF PHONOCARDIOGRAPHIC SIGNALS" MEDICAL AND BIOLOGICAL ENGINEERING AND COMPUTING,GB,PETER PEREGRINUS LTD. STEVENAGE, vol. 36, no. 3, 1 May 1998 (1998-05-01), pages 302-308, XP000751653 ISSN: 0140-0118 the whole document ---	33
A	US 5 795 304 A (LEE KAE YOL ET AL) 18 August 1998 (1998-08-18) column 6, line 12 -column 7, line 23 -----	1,3

INTERNATIONAL SEARCH REPORT

International application No.
PCT/GB 00/01675

Box I Observations where certain claims were found unsearchable (Continuation of item 1 of first sheet)

This International Search Report has not been established in respect of certain claims under Article 17(2)(a) for the following reasons:

1. ☐ Claims Nos.:
because they relate to subject matter not required to be searched by this Authority, namely:

2. ☒ Claims Nos.: 39 40
because they relate to parts of the International Application that do not comply with the prescribed requirements to such an extent that no meaningful International Search can be carried out, specifically:

see FURTHER INFORMATION sheet PCT/ISA/210

3. ☐ Claims Nos.:
because they are dependent claims and are not drafted in accordance with the second and third sentences of Rule 6.4(a).

Box II Observations where unity of invention is lacking (Continuation of item 2 of first sheet)

This International Searching Authority found multiple inventions in this international application, as follows:

see additional sheet

1. ☐ As all required additional search fees were timely paid by the applicant, this International Search Report covers all searchable claims.

2. ☐ As all searchable claims could be searched without effort justifying an additional fee, this Authority did not invite payment of any additional fee.

3. ☐ As only some of the required additional search fees were timely paid by the applicant, this International Search Report covers only those claims for which fees were paid, specifically claims Nos.:

4. ☒ No required additional search fees were timely paid by the applicant. Consequently, this International Search Report is restricted to the invention first mentioned in the claims; it is covered by claims Nos.:

1-16, 33-38

Remark on Protest

☐ The additional search fees were accompanied by the applicant's protest.

☐ No protest accompanied the payment of additional search fees.

FURTHER INFORMATION CONTINUED FROM PCT/ISA/ 210

This International Searching Authority found multiple (groups of) inventions in this international application, as follows:

1. Claims: 1-16, 33, 34-38

   Method and device for ECG analysis using wavelet transformation or matching pursuit algorithms and visually displaying the signal and/or the decomposed waveform.

2. Claims: 17-21

   Analysis of an ECG of a heart in ventricular fibrillation after commencement of CPR and method of disassociating the CPR signal from the heart signal.

3. Claims: 22-32

   Method of estimating the health of a heart in ventricular fibrillation in order to guide therapeutic intervention or to predict outcome.

FURTHER INFORMATION CONTINUED FROM PCT/ISA/ 210

Continuation of Box I.2

Claims Nos.: 39 40

Rule 6.2 (a)
References to Other Parts of the International Application
Claims shall not, except where absolutely necessary, rely, in respect of the technical features of the
invention, on references to the description or drawings. In particular, they shall not rely on such
references as: "as described in part ... of the description," or "as illustrated in figure ... of the
drawings."

The applicant's attention is drawn to the fact that claims, or parts of claims, relating to inventions in respect of which no international search report has been established need not be the subject of an international preliminary examination (Rule 66.1(e) PCT). The applicant is advised that the EPO policy when acting as an International Preliminary Examining Authority is normally not to carry out a preliminary examination on matter which has not been searched. This is the case irrespective of whether or not the claims are amended following receipt of the search report or during any Chapter II procedure.

INTERNATIONAL SEARCH REPORT

International Application No
PCT/GB 00/01675

Patent document cited in search report	Publication date	Patent family member(s)	Publication date
WO 9608992 A	28-03-1996	AU 3717495 A	09-04-1996
		EP 0869734 A	14-10-1998
		JP 11511036 T	28-09-1999
		US 5797840 A	25-08-1998
US 5439483 A	08-08-1995	NONE	
US 5795304 A	18-08-1998	NONE	